National Library of Canada
Bibliothèque nationale du Canada

Canadian Theses Service
Services des thèses canadiennes

Ottawa, Canada
K1A 0N4

# CANADIAN THESES

# THÈSES CANADIENNES

## NOTICE

The quality of this microfiche is heavily dependent upon the quality of the original thesis submitted for microfilming. Every effort has been made to ensure the highest quality of reproduction possible.

If pages are missing, contact the university which granted the degree.

Some pages may have indistinct print especially if the original pages were typed with a poor typewriter ribbon or if the university sent us an inferior photocopy.

Previously copyrighted materials (journal articles, published tests, etc.) are not filmed.

Reproduction in full or in part of this film is governed by the Canadian Copyright Act, R.S.C. 1970, c. C-30. Please read the authorization forms which accompany this thesis.

## AVIS

La qualité de cette microfiche dépend grandement de la qualité de la thèse soumise au microfilmage. Nous avons tout fait pour assurer une qualité supérieure de reproduction.

S'il manque des pages, veuillez communiquer avec l'université qui a conféré le grade.

La qualité d'impression de certaines pages peut laisser à désirer, surtout si les pages originales ont été dactylographiées à l'aide d'un ruban usé ou si l'université nous a fait parvenir une photocopie de qualité inférieure.

Les documents qui font déjà l'objet d'un droit d'auteur (articles de revue, examens publiés, etc.) ne sont pas microfilmés.

La reproduction, même partielle, de ce microfilm est soumise à la Loi canadienne sur le droit d'auteur, SRC 1970, c. C-30. Veuillez prendre connaissance des formules d'autorisation qui accompagnent cette thèse.

THIS DISSERTATION HAS BEEN MICROFILMED EXACTLY AS RECEIVED

LA THÈSE A ÉTÉ MICROFILMÉE TELLE QUE NOUS L'AVONS REÇUE

NL 339 (r. 86/01)

Canada

0-315-28224-X

35

National Library of Canada | Bibliothèque nationale du Canada

CANADIAN THESES ON MICROFICHE | THÈSES CANADIENNES SUR MICROFICHE

NAME OF AUTHOR/NOM DE L'AUTEUR Simon Peter Watkins

TITLE OF THESIS/TITRE DE LA THÈSE Isoelectronic Bound Excitons in Silicon

UNIVERSITY/UNIVERSITÉ Simon Fraser University

DEGREE FOR WHICH THESIS WAS PRESENTED/ GRADE POUR LEQUEL CETTE THÈSE FUT PRÉSENTÉE Master of Science

YEAR THIS DEGREE CONFERRED/ANNÉE D'OBTENTION DE CE DEGRÉ 1983

NAME OF SUPERVISOR/NOM DU DIRECTEUR DE THÈSE Professor M.L.W. Thewalt

Permission is hereby granted to the NATIONAL LIBRARY OF CANADA to microfilm this thesis and to lend or sell copies of the film.

The author reserves other publication rights, and neither the thesis nor extensive extracts from it may be printed or otherwise reproduced without the author's written permission.

L'autorisation est, par la présente, accordée à la BIBLIOTHÈQUE NATIONALE DU CANADA de microfilmer cette thèse et de prêter ou de vendre des exemplaires du film.

L'auteur se réserve les autres droits de publication; ni la thèse ni de longs extraits de celle-ci ne doivent être imprimés ou autrement reproduits sans l'autorisation écrite de l'auteur.

DATED/DATÉ 2 Feb 84 SIGNED/SIGNÉ

PERMANENT ADDRESS/RÉSIDENCE FIXE [redacted]

# ISOELECTRONIC BOUND EXCITONS IN SILICON

by

Simon P. Watkins

THESIS SUBMITTED IN PARTIAL FULFILLMENT OF

THE REQUIREMENTS FOR THE DEGREE OF

MASTER OF SCIENCE

in the Department

of

Physics

© Simon P. Watkins 1984

SIMON FRASER UNIVERSITY

May 1983

All rights reserved. This work may not be
reproduced in whole or in part, by photocopy
or other means, without permission of the author.

# APPROVAL

Name: Simon P. Watkins

Degree: Master of Science

Title of thesis: Isoelectronic Bound Excitons in Silicon

Examining Committee:

Chairman: B.P. Clayman

M.L.W. Thewalt
Senior Supervisor

J.C. Irwin

M. Plishke

R.F. Frindt
External Examiner
Professor
Department of Physics
Simon Fraser University

Date Approved: May 13, 1983

PARTIAL COPYRIGHT LICENSE

I hereby grant to Simon Fraser University the right to lend my thesis, project or extended essay (the title of which is shown below) to users of the Simon Fraser University Library, and to make partial or single copies only for such users or in response to a request from the library of any other university, or other educational institution, on its own behalf or for one of its users. I further agree that permission for multiple copying of this work for scholarly purposes may be granted by me or the Dean of Graduate Studies. It is understood that copying or publication of this work for financial gain shall not be allowed without my written permission.

Title of Thesis/Project/Extended Essay

Isoelectronic Bound Excitons in Silicon

Author:

(signature)

Simon Peter Watkins

(name)

2 Feb 84

(date)

## ABSTRACT

There has been a great deal of recent interest in a number of intense new photoluminescence lines observed in samples of Si doped with various impurities. This study details the results of transient photoluminescence measurements undertaken on several of these luminescence systems, in particular those associated with samples of Si doped with Be, Li, Cu, In, and Tl impurities. These measurements confirm that the lines are due to the recombination of excitons at isoelectronic binding centres. While the Si:Be and Si:Li centres fit into the previously observed systematics for isoelectronic binding centres in other host lattices, the unusual transient behaviour of the deep acceptor related Si:In and Si:Tl centres indicates a novel form of exciton binding centre hitherto unobserved in any other semiconductor host. The acceptor related data are analyzed in terms of a model in which excitons are bound to defects which can exist in one of two energetically inequivalent configurations separated by an energy barrier which determines the unusual temperature dependence of the spectral data.

TABLE OF CONTENTS

Approval ..... ii

Abstract ..... iii

List of Tables ..... v

List of Figures ..... vi

Acknowledgements ..... viii

I. Introduction ..... 1

Aims and Structure ..... 8

II. Experimental ..... 10

Light Sources and Spectral Methods ..... 10

Spectrometer and Optics ..... 13

Detection ..... 13

Cryogenics ..... 14

Electronics ..... 15

III. Examples of the J-J Coupling Model: Si:Be and Si:Li ..... 17

Si:Be Results ..... 17

Si:Li Results ..... 25

IV. Si:Cu Results ..... 29

V. Acceptor Related Results: Si:Tl and Si:In ..... 36

Experimental Results ..... 36

Si:Tl Transient Results ..... 39

Large Lattice Relaxation Model ..... 46

Si:In Transient Results ..... 51

VI. Summary and Conclusions ..... 60

VII. Appendix: Solution of Si:In Rate Equation ..... 62

References ..... 64

## LIST OF TABLES


| Table | | Page |
|---|---|---|
| 3.1 | Energies of no-phonon transitions in Si:Be | 19a |
| 4.1 | Line energies for Si:Cu centre | 31a |
| 5.1 | Si:Tl transient results | 42a |
| 6.1 | Si:In transient results | 53b |

LIST OF FIGURES


| Figure | | Page |
|---|---|---|
| 2.1 | Diagram showing typical pumping and collection optics | 12a |
| 2.2 | Response of the photomultiplier detector vs. wavelength | 13a |
| 2.3 | Block diagram of data aquisition system | 14a |
| 3.1 | Energy level diagram showing the splittings of the IBE ground state | 17a |
| 3.2 | Photoluminescence, absorption, and excitation spectra for Si:Be at three representative temperatures | 18a |
| 3.3 | Decay times for IBE in Si:Be vs. temperature | 20a |
| 3.4 | Photoluminescence spectra for Si:Li spectra | 25a |
| 3.5 | Decay times for IBE in Si:Li vs temperature | 26a |
| 4.1 | Photoluminescence spectrum of Si:Cu at 4.2K | 30a |
| 4.2 | Photoluminescence spectra of Si:Cu at three representative temperatures | 32a |
| 4.3 | Decay times of IBE in Si:Cu vs. temperature | 33a |
| 4.4 | Configuration coordinate diagram for a centre with large lattice relaxation | 34a |
| 5.1 | Comparison of Si:Tl and Si:In luminescence at 20K | 36a |
| 5.2 | Si:Tl spectra at various temperatures | 37a |
| 5.3 | Energy level diagrams for Si:Tl and Si:In centres | 38a |
| 5.4 | Spectra of Si:Tl and Si:In indicating strong coupling to phonon band | 38b |
| 5.5 | Transient luminescence curves for the Si:Tl A-centres at various temperatures | 39a |

Figure Page

5.6 Transient luminescence curves for the Si:Tl P-centres at various temperatures.....40a

5.7 Transient spectra of P and A-centres at 14 K on a linear scale.....40b

5.8 Possible configuration coordinate diagrams for the Si:Tl centre.....41a

5.9 Logarithm of the A to P changeover time constant vs. 1/T for Si:Tl.....42b

5.10 Subtracted P-centre decay curves showing the presence of two exponentials.....43a

5.11 Summary of Si:Tl transient data vs. temperature.....44a

5.12 Examples of large lattice relaxation models used in other semiconductor systems.....48a

5.13 Decay curves of two samples of Si:In at 4.2 K.....51a

5.14 Decay curves of Si:In at various temperatures.....52a

5.15 Subtracted Si:In decay curves indicating fast decay component.....52b

5.16 Summary of Si:In transient data vs. temperature.....53a

5.17 Ratio of Si:In luminescence decay prefactors as a function of temperature.....54a

## ACKNOWLEDGEMENTS

I would like to thank my supervisor, Dr. Mike Thewalt for his unflagging support, encouragement and guidance throughout this project. I am indebted to Tom Steiner for his electronic wizardry, without which much of the instrumentation used herein would have been unavailable. I would also like to thank Sara Swenson for her considerable efforts in proofreading and compiling the manuscript.

This work was supported by a grant from the National Sciences and Engineering Research Council of Canada. I am indebted to NSERC for a postgraduate scholarship.

## I. Introduction

The tremendous technological importance of crystalline Si as a device material has led to levels of purity and availability unrivalled by any other semiconductor. Si is therefore a very convenient material for the observation of a variety of low level impurity effects of interest to the solid state physicist. A clear example is the current revival in interest generated by the discovery of isoelectronic bound excitons (IBE) in this semiconductor.

Si is an indirect bandgap semiconductor with six two-fold spin degenerate conduction band minima at the $(0,0,\pm k_o)$ and equivalent points in k-space, where $k_o$ = 0.85 times the first Brillouin zone boundary wave vector. A single four-fold degenerate valence band maximum occurs at k = 0. Localized electron or hole states can be formed as packets of Bloch functions centred on the conduction or valence band extrema, with group velocity $\nabla E_k = 0$, and with the full symmetries and spin-orbit couplings of the energy bands from which they were derived. Dilute substitutional group V impurities such as P, with one extra nuclear charge, and all neighbouring bonds satisfied, can bind such a localized packet in a hydrogenic orbit with wave function:

$$\psi^{(i)}(r) = F^{(i)}(r)\ \psi(k^{(i)}, r)$$

where $\psi(k^{(i)},r)$ is the Bloch function at the band extremum and F(r) satisfies a simple effective mass equation. The effective electron mass is

a tensor quantity characterized by transverse and longitudinal masses, $m_T$ and $m_L$. The large effective dielectric constant, $\varepsilon = 11.4$, and small electron effective masses $m_L = 0.98m_o$ and $m_T = 0.19m_o$ imply a donor Bohr radius of ~10 nm. This ensures that the wavepacket is relatively localized in k-space to the order of $10^{-2}$ times the Brillouin zone boundary wave vector. In addition, group III acceptors such as Al, with one less nuclear charge, can bind a hole in a localized hydrogenic orbit.

A free exciton corresponds to a hydrogenic bound state between hole and electron states. In indirect bandgap semiconductors such as Si, radiative recombination of the free exciton, or of any electron and hole at their band extrema, involves emission of a crystal momentum conserving phonon in addition to a photon of energy slightly less than the bandgap. This has the effect of greatly reducing the transition probability compared with direct gap semiconductors. In 1958, Lampert[1] predicted the existence of the bound exciton, consisting of an electron-hole pair bound to a neutral donor in a four particle bound state (three mobile particles and a fixed impurity ion), somewhat analogous to the $H_2$ molecule. This was subsequently observed by Haynes in 1960.[2]

The above cases are ideal in the sense that they involve predominantly long range Coulomb interactions only. Since P and Si share the same core electron structure, the P donor ion can be treated to a very good approximation as a point positive charge in an otherwise perfect Si lattice. The observed levels of the P donor[3] agree well with the effective mass theory predictions based on the work of Kohn and Luttinger.[4] Most other group V donors however, show large deviations from these values[3], with similar trends in group III acceptors.[5] In addition to the long range

Coulombic potential of the ideal donor, these impurities introduce a short range attractive or repulsive potential due to the perturbation caused by the differences in the core electron structure. The difference between the host lattice self-consistent potential in the absence of the impurity and that introduced by the defect is known as the central cell potential and typically has a range the order of a lattice spacing. The large resulting deviations from the effective mass predictions of the binding energies, due to the localized attractive or repulsive short ranged potential, are the hallmark of deep states, to which effective mass theory no longer applies. Such states are substantially localized in real space to the order of a lattice constant and hence mix Bloch states from throughout the entire Brillouin zone.

The possibility of an exciton binding to an impurity substituting isoelectronically for the host lattice was first recognized by Thomas et al. in 1965[6] for the case of GaP:Bi. In a subsequent paper based on measurements on ZnTe:O and GaP:Bi, Hopfield, Thomas, and Lynch[7] proposed that isoelectronic binding was possible if the impurity first localized one particle in a short range localized defect state, binding the second particle in the long range Coulomb potential which this would introduce. Such systems were designated isoelectronic donors or acceptors depending on whether the hole or electron was bound first.

The model had immediate success in explaining the spectral data in terms of j-j coupling of the electron and hole, as well as determining the relative oscillator strengths of these levels based on the phonon couplings of the tightly bound particle.

A primary implication of this model is the breakdown of the crystal momentum conservation condition for recombination. Since the tightly bound particle mixes states from the entire Brillouin zone, a strong no-phonon line is prominent in most absorption and luminescence spectra.

The Hopfield, Thomas, Lynch model has been directly confirmed in GaP:Bi by Dean et al.[8] who observed pair spectra due to recombination between a bare hole bound to the Bi centre and various shallow group VI donors. Other evidence is given by the usual discrepancy between the spectroscopically determined binding energy and the dissociation energy of the complex based on thermal quenching of the luminescence. This is usually interpreted as indicating the ionization of the weakly bound particle, leaving the other still tightly bound by the central cell potential of the impurity. Theoretical calculations[9] of the binding energies based on the difference between the host and impurity pseudopotentials, have given reasonable qualitative predictions as to which single atom isoelectronic dopants should produce bound states. In particular, no IBE are predicted for the case of single atom isoelectronic substitutional dopants in Si.

The high degree of localization of the first bound particle can be responsible for a considerable degree of lattice distortion relative to the bare isoelectronic centre. This lattice relaxation is familiar from the study of optical transitions in other solids, and is responsible for a strong coupling to vibrational sidebands in the form of phonon replicas which couple both to the continuum of acoustic phonons, and to "in-band" modes of the defect centre. These phonon replicas are observed in addition to the momentum conserving transverse optic (TO), transverse acoustic (TA), and longitudinal optic (LO) lattice phonon replicas expected from an

indirect bandgap semiconductor.

In practice, transient luminescence measurements give a convenient means of identifying isoelectronic defects. In 1966, Nelson et al.[10] demonstrated that Auger emission was the dominant decay channel for donor or acceptor bound excitons in GaP, based on the large discrepancy between the observed luminescence lifetime and the transition probability calculated on the basis of absorption measurements. This recombination mechanism, in which the energy of the recombining electron and hole is transferred to the third particle as kinetic energy, is not available to the IBE, which consists of only two bound particles. In practice, this results in IBE decay times up to $10^3$ times greater than those of ordinary bound excitons for a given host lattice [10]. In addition, Cuthbert and Thomas[11] have explained the temperature dependence of the decay time of IBE in GaP:Bi and ZnTe:O in terms of the previously mentioned j-j coupling model. In this model, j-j coupling between a $j = 1/2$ electron and a $j = 3/2$ hole gives rise to a splitting of the exciton ground state transition, of which the lowest lying level, being dipole forbidden, dominates the decay rate at low temperatures.

Considering that it was in Si that Haynes first observed ordinary bound excitons in 1960[2], it is ironic that evidence of isoelectronic bound excitons was not observed in this host until 1979 by Weber et al.[14] Since then, numerous new IBE photoluminescence lines have been discovered in samples of crystalline Si using various sample preparation techniques.[14-32] Whereas previously reported values of bound exciton lifetimes in Si have been of the order of nanoseconds [12,13], these new centres have lifetimes between 50 μs and 4 ms. The extremely long lifetimes of these centres,

together with their high radiative quantum efficiencies and strong coupling to non - momentum - conserving phonons, provide ample evidence of isoelectronic binding. In all cases but Si:Be and Si:Li, these centres are present in concentrations so low that absorption measurements have not been possible to date. None of the binding centres appears to be of the simple substitutional variety observed in other semiconductors and, except for the case of Si:Be, the precise trap constituents remain a mystery.

Weber et al.[14,15] observed a triplet of long-lifetime lines from an undetermined centre in samples of Al doped Si, which they labelled A,B,C. The thermalization behaviour of these spectral lines, as well as the temperature dependence of their decay rates, was similar to that encountered in isoelectronic binding centres in other semiconductors.

Rostworowski and Parsons[16] reported a similar set of lines, D1 - D4, in samples of neutron damaged, ultra-high purity Si, with lifetimes as long as 60 to 70 μs at liquid He temperatures. In both of the above examples, the nature of the binding centres is still considered a complete mystery.

Henry et al.[17] have observed intense lines in samples of Be doped Si, which show behaviour similar to the above centres, but for which the trapping centre has been identified as a Be-Be pair. This centre is unique among the IBE observed in Si to date, in that absorption measurements can be made on it, which suggests a much higher concentration of binding centres. On the basis of the strong coupling of the low-lying levels to low energy acoustic phonons, they postulated that the centre is an isoelectronic donor, i.e. the electron is loosely bound in a Coulombic manner to the more tightly bound hole.

Another centre which appears to show the typical j-j coupling behaviour was observed by Canham et al.[18] in samples of electron irradiated Li doped Si. From detailed isotope doping studies, it was concluded that the binding centre consists of four Li atoms.

While all of the above binding centres appear to show the expected IBE behaviour predicted by the Hopfield, Thomas, Lynch model, this is not the case for the systems of intense photoluminescence lines observed in samples of Si doped with the deep acceptors In and Tl.[19-27] The In related lines were first observed by Vouk and Lightowlers[19], but it was Mitchard et al.[20] who demonstrated the long decay times of the centres ( 200 μs), indicative of some type of isoelectronic binding centre. They concluded that the three intense lines, P,Q,R, were due to different binding centres, but subsequent studies based on lifetime and thermal activation measurements have shown that they all originate from the same centre.[22-24]

The discovery by Thewalt et al.[22] and Weber et al.[23] of the huge enhancement in luminescence intensity obtained by a rapid quench of the samples from high temperatures (800 - 1200 K), has greatly facilitated the study of these centres.

In order to determine whether the central cell potential of In was important in the P,Q,R binding centre, Thewalt et al.[26] applied the same heat treatment to samples doped with the even deeper acceptor, Tl. The result was a series of lines with a striking resemblance to those observed in Si:In, but displaced to lower photon energy by 67.4 meV. In contrast to the P,Q,R lines in Si:In however, these were replaced by a series of higher energy lines, A,B,C etc., upon cooling below 12 K. The thermally activated changeover was completely reversible, and led to a model in which

the binding centre could exist in one of two energetically different configurations separated by an energy barrier. Evidence of the simple j-j coupling scheme was absent in both of these binding centres. In addition, the centres show rather anomalous coupling to local mode and lattice phonons.

## Aims and Structure

This thesis includes the results of spectral and time resolved luminescence measurements on several new isoelectronic binding centres in Si. The analysis of the material has been divided into three sections, each of which emphasizes a different aspect of isoelectronic binding centres in Si. Chapter 2 deals exclusively with experimental methods. Chapter 3 deals with new photoluminescence lifetime and spectral data on Si:Be and electron irradiated Si:Li, which conclusively demonstrate the isoelectronic nature of these centres. The temperature dependence of the decay time is fitted accurately to the standard j-j coupling scheme for IBE . In addition, the Si:Be lifetime data, together with absorption measurements, are used to determine for the first time, the concentration of an isoelectronic defect in Si.

In addition to a strong principal set of lines, a set of weaker lines are also seen at higher energies in both samples and have been ascribed tentatively to a lowering of the IBE central cell potential by nearest neighbour substitutional C impurities in analogy to the recent

model for the so-called X-centre acceptors.[38]

Chapter 4 includes spectral and decay time measurements on the Si:Cu system, which offer direct evidence of isoelectronic behaviour. The centre shows a strong coupling to a complex band of local mode and lattice phonon replicas typical of a centre with strong lattice relaxation. Chapter 5 deals exclusively with the novel results of transient measurements on the Si:In and Si:Tl isoelectronic centres. The Si:Tl data is presented in terms of a model in which the binding centre can exist in one of two configurations separated by an energy barrier. The Si:In data is treated with the same model, but different assumptions are made regarding the relative energies and barrier heights. A detailed rate equation analysis of the data is performed. Such a system appears to be unique in the literature of semiconductor defects.

Much of the data presented here has been previously published or accepted for publication.[28-30]

## II. Experimental

### Light Sources and Spectral Methods

Three different spectroscopic techniques were used to obtain the data presented in this study. In photoluminescence measurements, the pump photon energy $h\omega$ is fixed, either to any value above the bandgap, or to a resonant energy level of the system being examined, and the luminescenece intensity is scanned as a function of wavelength. Luminescence is emitted from each level in proportion to its thermal occupation. All photoluminescence measurements reported here were performed with above bandgap excitation. In this scheme, free carriers are generated by shining light of energy greater than the bandgap $E_g$ into the sample. The free carriers thermalize down to the band extrema in times of the order of $1 \times 10^{-12}$ s. Formation of energetically favourable bound states such as free excitons, bound excitons, bound multi-exciton complexes, IBE, and electron hole droplet, occurs on the order of nanoseconds. A disadvantage of above bandgap excitation is that some of the above decay channels can lead to a non-constant IBE generation rate as a function of temperature by competing for free e-h pairs. This can complicate the study of thermally activated processes in which the IBE population is inferred from the luminescence intensity. The advantage of this method is that any source with photon energy $h\omega > E_g$ can be used. For this project, the principle sources for above gap excitation were two high power ion lasers, $Ar^+$ and $Kr^+$, with the

most useful lines at 514.5 nm (8 W maximum power) and 676.4 nm (3 W maximum power) respectively. In addition many of the transient results were obtained using a liquid nitrogen - cooled pulsed GaAs laser diode array operating at 870 nm. Since the absorption of the pump beam is a strongly increasing function of the pump energy, the GaAs laser was the preferred source for bulk excitation of the samples when low signals were encountered.

A disadvantage of photoluminescence measurements is that they are generally confined to the ground state and the lowest lying excited states since the centres often dissociate at the temperatures required for the thermal occupation of the higher energy excited states. This disadvantage is avoided in absorption and excitation spectroscopy, in which the pump frequency is varied across the resonant absorption peaks of the system. In both techniques, tunable light was supplied by means of a blackbody source, either a 500 W tungsten halogen lamp or a 1 kW Xe arc lamp, in conjunction with a single 3/4 m spectrometer. A two beam absorption technique was used in this study, in which the pump beam was split into two components; one was passed through the sample and the other served as a reference beam. The two beams were then alternately chopped by means of a chopper wheel and made incident on the detector. The resulting signal was fed into a lock-in amplifier, which was nulled away from the absorption peaks by inserting a pair of polarizers in front of the reference beam. Excitation spectra were obtained by resonantly pumping into the various exciton levels at low temperatures and monitoring the luminescence intensity at the ground state transition. At the temperatures at which these measurements were made ($T < 2$ K) all IBE which are created by resonant absorption into the

excited states thermalize down to the ground state in a time short compared to any of the IBE radiative lifetimes.

Initially, transient measurements were achieved by chopping the output of one of the ion lasers by means of a high speed mechanical chopper wheel. By operating at speeds in the vicinity of 5000 rpm, and focussing the beam at the chopper blades, rise times of the order of 10 μs were attainable, which was more than adequate for the Si:Be and Si:Cu measurements. A Si PIN photodiode provided the start pulse for the data aquisition electronics.

Another technique used subsequently in some of the Si:In measurements, and which resulted in rise and fall times of less than 5 μs, involved the use of the electro-optic modulator in a commercially built Harris mode locker head in conjunction with the $Kr^+$ ion laser. By detuning the laser cavity length such that the rf frequency applied to a resonance of the acousto-optic modulator was far from the mode spacing frequency of the laser, it was possible to completely inhibit lasing by the application of sufficient power. Switching of the laser beam was then achieved by switching the rf power off and on. Application of the rf power effectively coupled enough light out of the cavity that the laser fell below threshold.

The GaAs diode array was switched by means of a fast, high current MOS power transistor. This source provided pulses of 300 ns width, and rise and fall times of 50 ns, which was more than sufficient for the Si:Tl measurements.

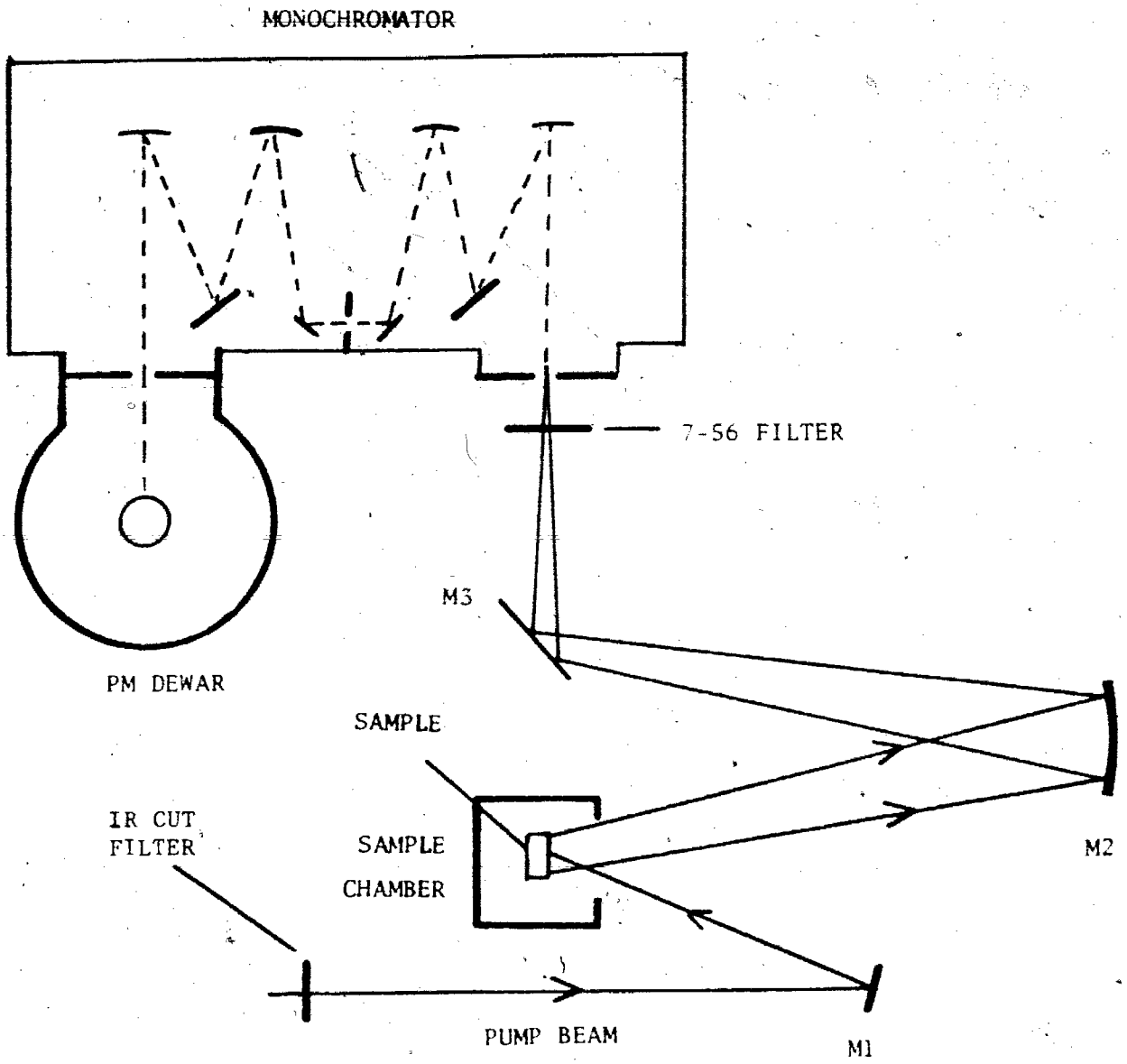


Fig. 2.1

Diagram showing typical pumping and collection optics.

## Spectrometer and Optics

Fig 2.1 shows a typical pump beam and collection optics arrangement used in many of the photoluminescence measurements. Due to the large angular spread ( $30^{o}$) in the GaAs emission, additional focussing optics were required for this source. Luminescence light was collected by means of a 6" diameter, 11" focal length concave mirror, and focussed on the entrance slits of a Spex Czerny-Turner double spectrometer with 600 lines/mm gratings, blazed for 1 μm. The purpose of the infrared cut filter in Fig. 2.1 was to eliminate the possibility of overloading the photomultiplier tube with spurious atomic luminescence lines and plasma discharge light from the ion laser tube. The 7-56 visible cut filter was used to eliminate the possibility of saturating the tube with pump light feedthrough in the second order of the spectrometer grating.

## Detection

The chief detector used in this study was a Varian VPM159A photomultiplier tube with enhanced response in the near infrared. This tube has an InGaAsP photocathode with a rated quantum efficiency of ∿1% at 1.1 μm. The sharp drop-off in spectral response beyond 1.1 μm is shown in Fig. 2.2. A dark count of ∿30 counts per second is achieved by cooling the detector to $-100^{o}C$ with a closed cycle refrigeration unit.

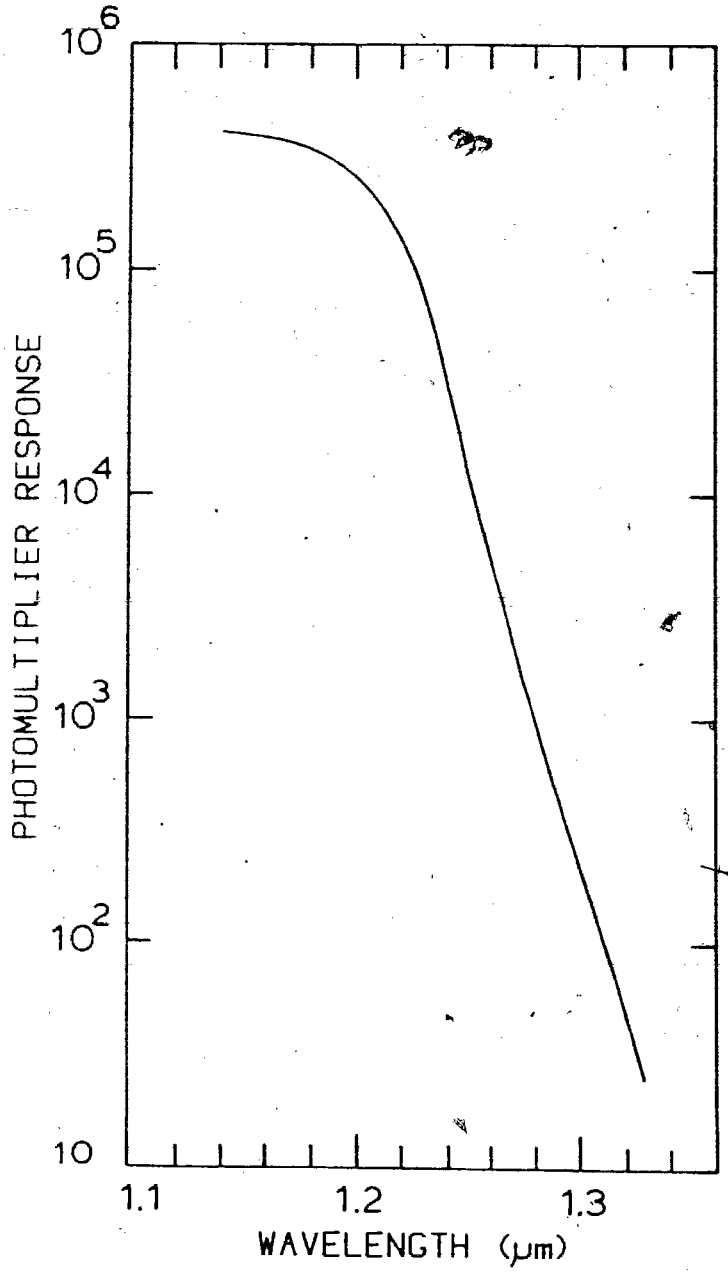


Fig. 2.2

Response of the photomultiplier detector vs. wavelength.

Some of the data reported here were obtained using the Ge detector spectrometer system in Dr. R.R. Parsons optics laboratory. This system extended the available wavelength to 1.7 um.

## Cryogenics

All photoluminescence measurements were made at temperatures below 70 K using liquid or gaseous He as the cryogen. For temperatures below 4.2 K, samples were mounted in the immersion tail of a large magnet dewar. A large pumping port enabled temperatures as low as 1.2 K to be achieved. Temperature control was achieved by regulating the pumping pressure. For temperatures above 4.2 K, a smaller variable temperature dewar was used, in which the sample was cooled by gas flow from a liquid He reservoir. The samples were mounted on a resistively heated Cu block, regulated by means of an electronic temperature controller which employed a Si diode temperature sensor. Thermal contact was achieved by pressing the samples into a stress free In pad soldered directly to the temperature control block. This configuration allowed stable regulation from 7 K to room temperature. Temperatures between 4 K and 7 K were achieved by pumping on the sample chamber. This technique was not as stable as operating at atmospheric pressure, but reasonable regulation was still possible.

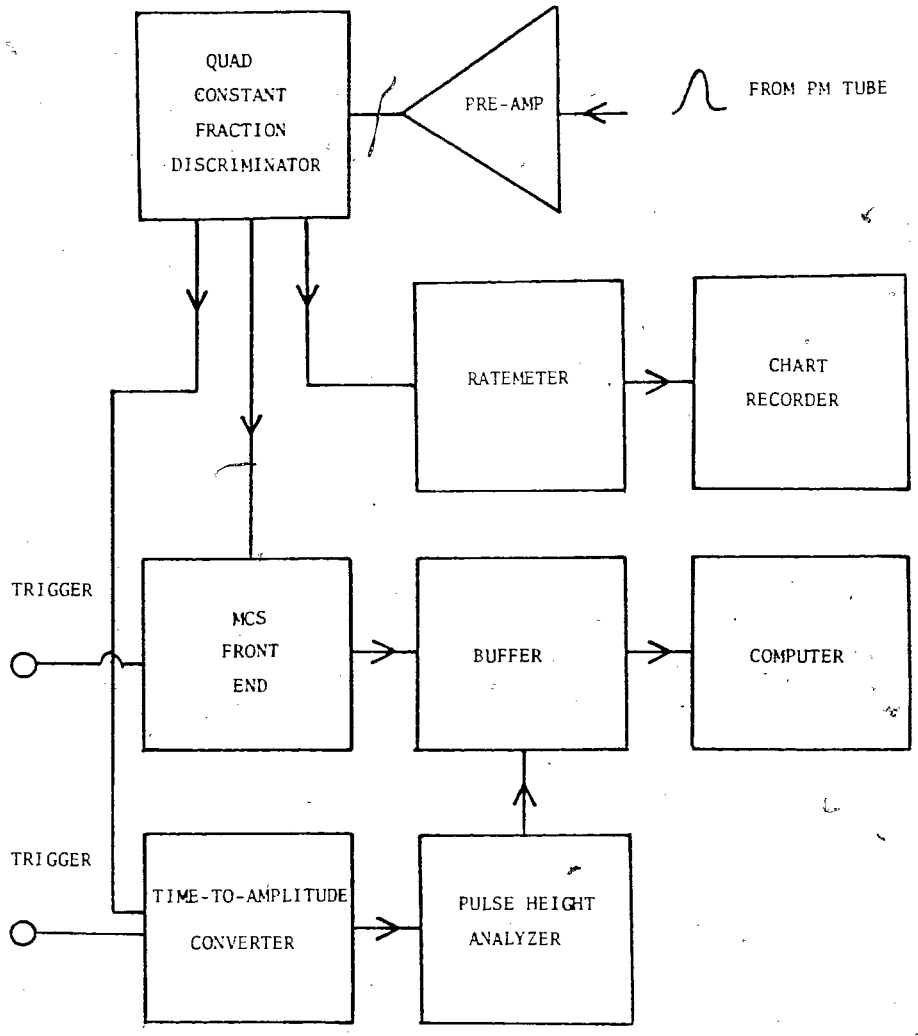


Fig.- 2.3

Block diagram of data aquisition system.

## Electronics

A block diagram of the main features of the experimental systems used in this study is given in Fig. 2.3. Photoluminescence measurements were processed in the photon counting mode. Spectral scans were recorded on a strip chart recorder using a synchronous motor drive to advance the spectrometer. Calibration markers were inserted as required by zeroing the recorder at the appropriate spectrometer readout settings.

For lifetimes greater than 1 μs, multichannel scaling is the most convenient method of measuring photoluminescence decay times. In this mode of operation, photon pulses are sorted into successive discrete 'bins' of a given interval called the dwell time, beginning from some given start time, defined in this case by the start of the pump pulse. Initially, transient measurements were obtained with a Tracor Northern TN-1750 multichannel analyzer with a minimum dwell time of 10 μs per channel and a maximum of 4K channels in the multichannel scaler mode. The multichannel scaler was triggered from the rising edge of the repetitive pump pulse train. Subsequent higher resolution measurements on the Si:Tl and Si:In luminescence systems were made possible by the availability of an improved multichannel analyzer system, controlled by means of an IBM personal computer, and capable of achieving a minimum dwell time of 1 μs. In addition, for lifetimes shorter than 1 μs, it was possible to operate this system in pulse height analyzer mode. In this arrangement, the time interval between the start of the pump pulse and the detection of a photon is converted into an analog voltage level by a time-to-amplitude converter. This is then fed into the pulse height analyzer, which generates a

histogram of counts versus voltage. If the number of luminescence photons detected per pump pulse is less than unity, an undistorted transient spectrum is obtained. This is not a severe restriction in practice, given the high repetition rates which are useable when measuring such short lifetimes. The advantage of this system is that extremely high time resolutions, down to the sub-nanosecond range, are possible.

Transient data were analyzed directly by the computer using a variety of routines which permitted least squares fitting to exponential decay curves, background subtraction, and other user programmable operations.

## III. Examples of the J-J Coupling Model: Si:Be and Si:Li

### Si:Be Results

Diffusion of the group II impurity Be into Si was observed by Henry et al.[17] to produce a set of intense photoluminescence lines with three thermalizing no-phonon components near 1078 meV, reminiscent of those from isoelectronic binding centres observed in other semiconductors. On the basis of detailed Zeeman studies[31], combined with previous transport measurements[33], the lines were attributed to the binding of an exciton at an "interstitialcy" consisting of two Be atoms sharing a single substitutional site. Such a defect would satisfy all neighbouring bonds with the surrounding lattice and can be viewed as a nearest neighbour double donor - double acceptor pair. Henry et al.[17] explained the thermalization of the lines in terms of a simple j-j coupling model previously applied to isoelectronic binding centres in other materials. The main features of this coupling scheme are given below, since the explanation of the transient data presented here is in terms of this model. Kohn and Luttinger[4] have shown that an effective mass 1s state formed from Bloch functions centred on the six equivalent conduction band minima of Si is split by the $T_D$ crystal field into three levels, the lowest of which, with the inclusion of spin-orbit coupling, resembles an $S_{\frac{1}{2}}$ atomic state, and transforms as the $\Gamma_6$ representation of the $T_D$ point group. In all semiconductors with cubic symmetry, hole states transform as $P_{\frac{3}{2}}$- like $\Gamma_8$

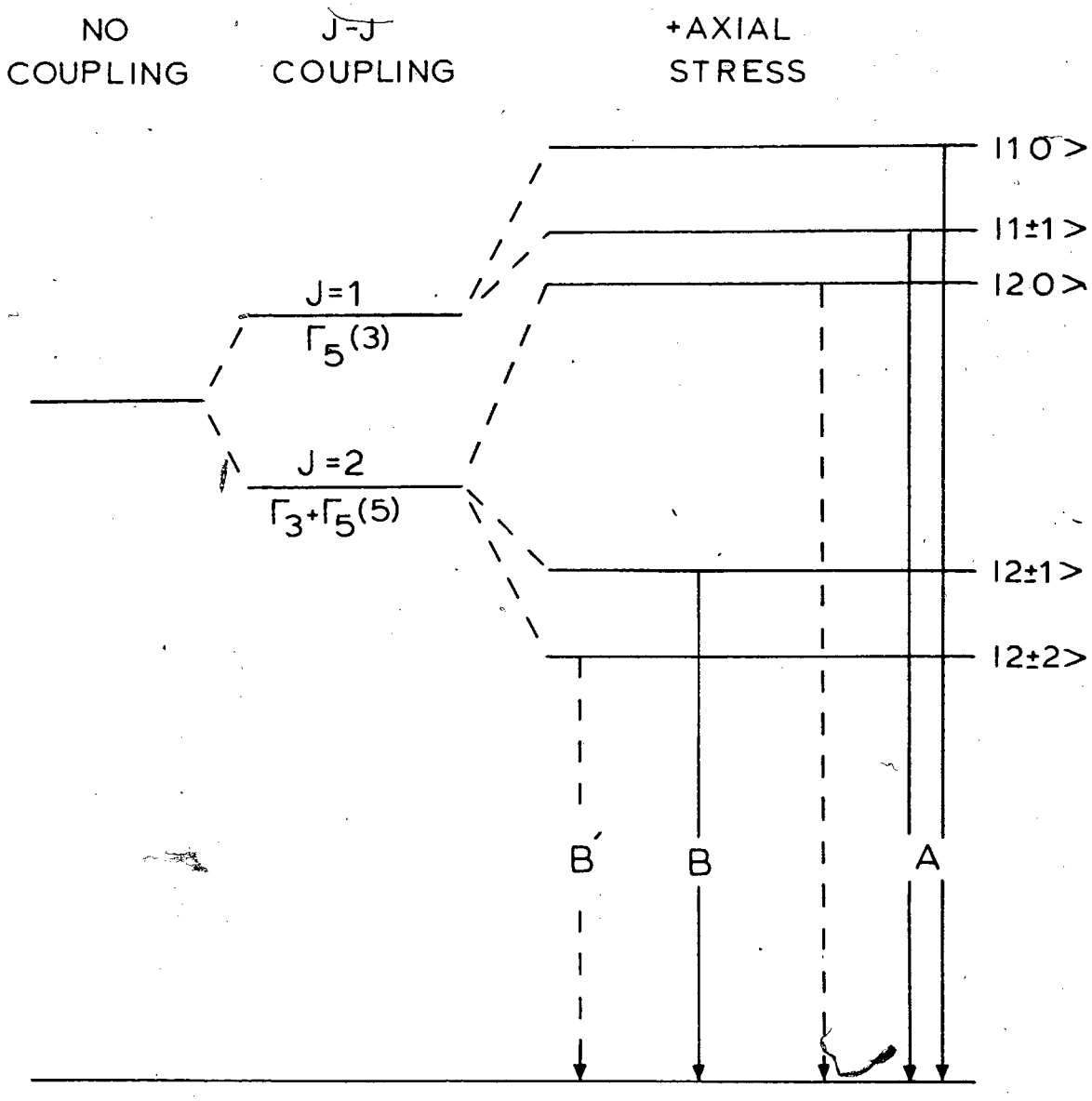


Fig. 3.1

Energy level diagram showing the splitting of the IBE ground state (a) in the absence of j-j coupling, (b) in the presence of j-j coupling alone, and (c) with both j-j coupling and internal strain due to an axial binding centre. The vertical lines represent possible recombination transitions, with solid lines denoting dipole allowed transitions and dashed ones those which are dipole forbidden. The A, B, B' notation represents an explanation of the Si:Be spectrum within this model.

states. By group theory , the full exciton state transforms as the direct product of the electron, hole, and is envelope representations, $\Gamma_6 \times \Gamma_8 \times \Gamma_1 = \Gamma_3 + \Gamma_4 + \Gamma_5$ . Morgan and Morgan [34] have shown that this is equivalent to combining states with angular momentum j = 1/2 and j = 3/2 to form a five-fold degenerate J = 2 state transforming as $\Gamma_3 + \Gamma_4$ and a three-fold degenerate J = 1 state transforming as $\Gamma_5$. The $T_D$ crystal field is not observed to cause any splitting of the J = 2 state.[34] The degeneracy between the the J = 1 and J = 2 states is split by the Coulomb interaction between the electron and the hole (see Condon and Shortley[35] on combining atomic states with j = 1/2 and j = 3/2 in the j-j coupling regime). Since the electron and hole have opposite signs, the ordering of the levels is the opposite of the atomic case, and the J = 2 state lies below the J = 1 state (Fig 3.1). Dipole selection rules forbid the transition from the J = 2 exciton state to the J = 0 crystal ground state. The effect of an axially symmetric binding centre is to split the degeneracy of the magnetic substates, $|j \pm m_j\rangle$ as shown in Fig 3.1. The axial field causes mixing of the $|2 \pm 1\rangle$ states with the $|1 \pm 1\rangle$ states from the allowed levels, thus relaxing the selection rules somewhat for transitions from this substate. The $|2 \pm 2\rangle$ ground state is not mixed with any of the J = 1 states, resulting in a very low oscillator strength for this transition.

The experimental measurements undertaken on Si:Be were obtained with samples of Be diffused, float zone refined Si supplied by Dr. E.C. Lightowlers and prepared by means of a diffusion technique described previously.[17] Typical Si:Be photoluminescence spectra obtained with the $Ar^+$ laser are shown in Figs. 3.2c,d,e for three representative temperatures.

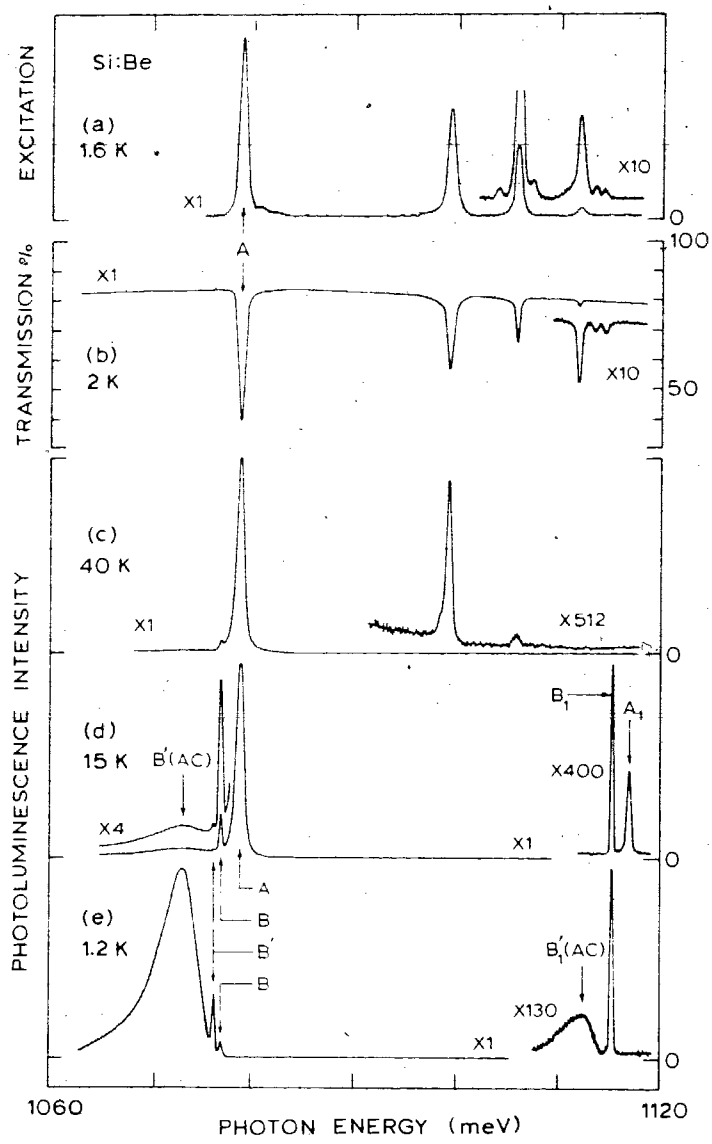


Fig. 3.2

(a) An excitation spectrum at 2K measuring the intensity of the B'(AC) luminescence as a function of pump beam energy. (b) A background corrected absorption spectrum obtained with a 3mm thick sample. Both (a) and (b) show the dominant A line as well as a series of excited states with monotonically decreasing oscillator strengths. Luminescence spectra are shown in (c), (d), and (e) for three representative temperatures. The main series A, B, B', and B'(AC) shows the standard IBE j-j coupling thermalization behaviour. In addition, a weaker set, $A_1$, $B_1$, and $B'_1$(AC) are observed at higher energies and show the same thermalization behaviour.

The relevant energies are summarized in table 3.1. Following the interpretation of Henry et al.[17], the strong higher temperature line, labelled A is ascribed to an unresolved doublet corresponding to an allowed transition from the two J = 1 sublevels of an IBE. The more weakly allowed B line, ascribed to the $|2\pm1\rangle$ sublevels dominates the luminescence at intermediate temperatures as the A level becomes depopulated. Finally, at very low temperatures, when all other levels are depopulated, the B' line, and its broad band of acoustic phonon replicas, B'(AC), dominate the luminescence, corresponding to "dipole forbidden" transitions from the $|2\pm2\rangle$ level, resulting in a drastic decrease in the oscillator strength at low temperatures. The above designations have been confirmed by Henry et al.[17] and by Killoran et al.[31] on the basis of detailed Zeeman and uniaxial stress analysis.

In addition to the strong A,B,B' luminescence system observed near 1078 meV, a set of much weaker lines, denoted $A_1$,$B_1$,$B_1$'(AC) are observed near 1117 meV (Figs. 3.2c,d,e). The thermalization behaviour of these lines is similar to that of the A,B,B' lines with the difference that the equivalent of the B' no-phonon line, $B_1$', was not apparent in the spectra obtained with the $Ar^+$ laser (subsequent measurements obtained using GaAs bulk excitation have indeed shown a very weak no-phonon line, $B_1$', at 0.6 meV below $B_1$). These weaker lines were initially ascribed to acceptor bound exciton luminescence centres by Henry et al.[17], but the transient and spectral studies undertaken as part of this project show isoelectronic behaviour similar to that of the stronger A,B,B' centres.

The implications of the j-j coupling model with regard to the temperature dependence of the IBE decay rates are straightforward to

Table 3.1

Energies of No-Phonon Transitions in Si:Be
(in order of decreasing energy)

| Transition | | E(meV) | |
|---|---|---|---|
| $A_1$ | | 1117.0 | ± 0.1 |
| $B_1$ | | 1115.21 | ± 0.05 |
| $B_1'$ | | 1114.53 | ± 0.05 |
| excited | *w* | 1114.3 | ± 0.1 |
| states | *w* | 1113.42 | ± 0.1 |
| of | *m* | 1111.89 | ± 0.08 |
| principal | *w* | 1107.1 | ± 0.15 |
| isoelectronic | *s* | 1105.68 | ± 0.08 |
| bound | *w* | 1103.2 | ± 0.15 |
| exciton | *s* | 1099.16 | ± 0.08 |
| A | | 1078.27 | ± 0.08 |
| B | | 1076.34 | ± 0.05 |
| B' | | 1075.74 | ± 0.05 |

*w* ≡ weak, *m* ≡ moderate, *s* ≡ strong

calculate. Assume that a population of excitons N is created at t = 0 by a laser pulse. Since the time required to reach thermal equilibrium is very short ( $10^{-12}$-$10^{-14}$ s) compared with the observed exciton decay rate (in the range of ms to μs for most isoelectronic centres), one may assume thermal equilibrium at all times. The population at any given time in the ith level is given by:

$$N(t)\ g_i\ \frac{e^{-E_i/kT}}{Z} \tag{1}$$

where N(t) is the total number of excitons, $g_i$ and $E_i$ are the degeneracies and the energies of the ith level, and:

$$Z = \sum_i g_i\ e^{-E_i/kT}$$

The total decay rate is therefore given by

$$\frac{dN(t)}{dt} = \frac{N(t)}{Z} \sum_i g_i\ \frac{e^{-E_i/kT}}{\tau_i} \tag{2}$$

where $\tau_i$ is the radiative lifetime of the ith state. This treatment neglects the possibility of nonradiative decay channels, which would seem a reasonable assumption at these low temperatures, given the low population of thermal phonons. Fig. 3.3 summarizes the results of A,B,B' and $A_1$,$B_1$,$B_1$' luminescence lifetime measurements obtained in the temperature range from 1.2 to 60 K using mechanically chopped $Ar^+$ laser excitation. The transient data for both the A,B,B' and the $A_1$,$B_1$,$B_1$' systems show a similar temperature dependence. Within each luminescence system, the lifetimes of

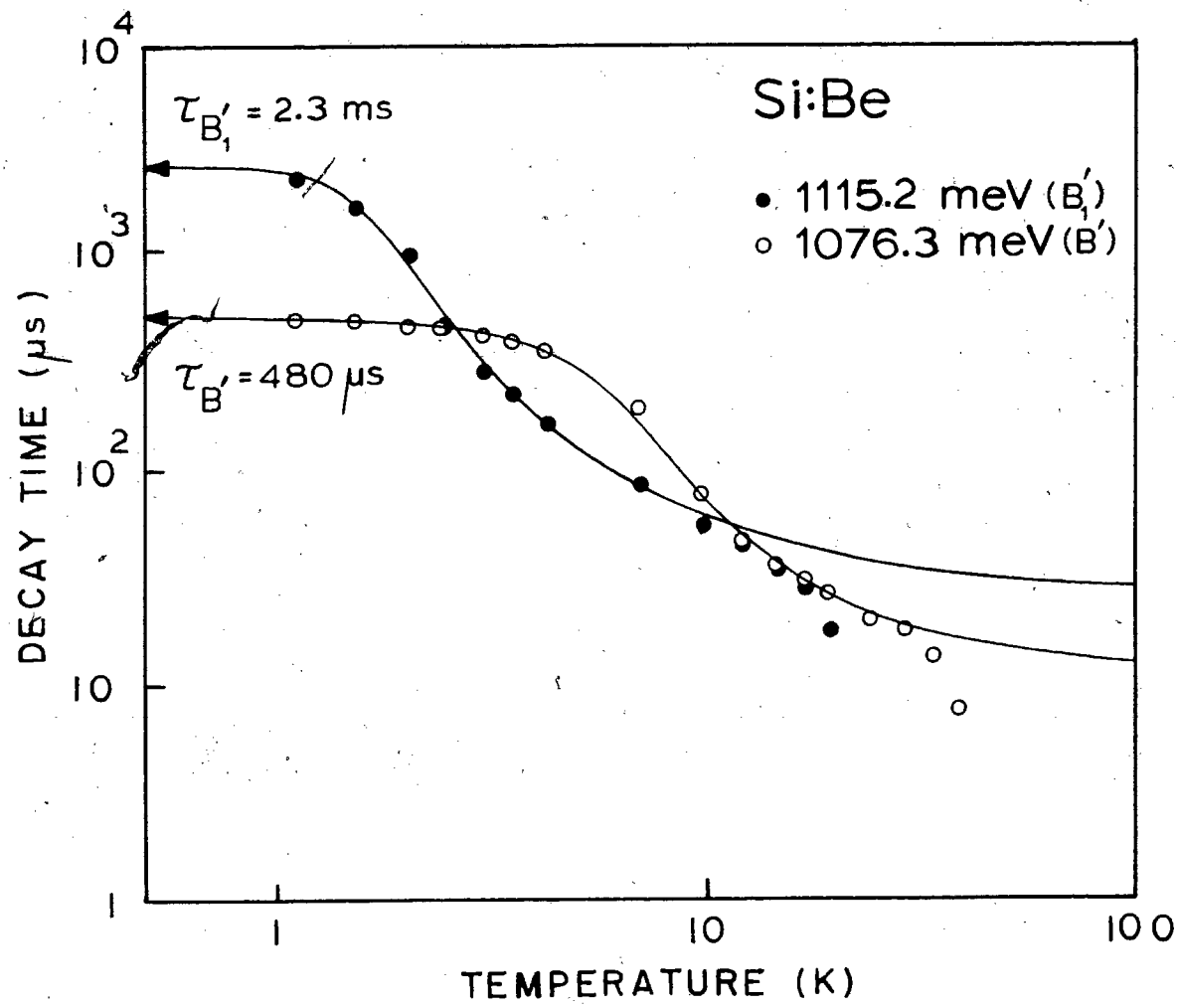


Fig. 3.3

The measured lifetimes for the two IBE centres in Si:Be as a function of temperature. The solid lines represent the best fits using the expressions given in the text. The deviation at high temperatures is due to the thermal dissociation of the bound excitons.

all lines were observed to be the same, confirming that only two independent binding centres were present. The very long lifetimes confirm the isoelectronic nature of both systems. At low temperatures, both sets of lines are seen to have very long decay times as expected, due to the depopulation of the higher lying dipole allowed transitions. As the temperature is increased, the lifetime decreases as the higher lying levels become thermally populated, reaching a plateau corresponding to the high temperature occupation limit of the upper levels. The rapid decrease in lifetime at temperatures above 40 K is ascribed to thermal breakup of the excitons, and is familiar from a variety of other binding centres.[11,15,20] The solid lines in Fig 3.3 represent the best fits to the lifetime data using the following expression based on equation (2):

$$\tau = \frac{\left(1 + \frac{g_2}{g_1} e^{-E_2/kT} + \frac{g_3}{g_1} e^{-E_3/kT}\right)}{\left(\frac{1}{\tau_1} + \frac{g_2}{g_1\tau_2} e^{-E_2/kT} + \frac{g_3}{g_1\tau_3} e^{-E_3/kT}\right)} \qquad (3)$$

Here, $\tau$ is the total decay time, $\tau_1$, $\tau_2$, and $\tau_3$ are the radiative lifetimes of excitons in the $B'(B_1')$, $B(B_1)$ and $A(A_1)$ states respectively, $g_1$, $g_2$ and $g_3$ are the corresponding degeneracies of these levels, and $E_2$ and $E_3$ are the ground state energies of the B and A lines relative to the zero defined by the level responsible for the $B'(B_1')$ transitions. Following Henry et al.[17] the degeneracies are taken as $g_1 = g_2 = 2$ and $g_3 = 3$ (see Fig. 3.1). For the dominant low energy A,B,B' centre, the values of $E_2 = 0.60$ meV and $E_3 = 2.53$ meV were derived fom the observed spectroscopic splittings. The best fit was then obtained with $\tau_1 = 480$ μs, $\tau_2 = 180$ μs

and $\tau_3 = 4.6\ \mu s$. For the higher energy $A_1, B_1, B_1'$ centre, the spectroscopic separations relative to the no-phonon line $B_1'$, hereafter denoted $E_2'$ and $E_3'$, were not available at first, due to an initial inability to see the line with $Ar^+$ excitation. Therefore, for this system $E_2'$ was also taken as an adjustable parameter, with $E_3'$ constrained by the observed spectroscopic splitting $E_3'-E_2' = 1.8$ meV. The best fit was then obtained with $E_2' = 0.68$ meV, $\tau_1 = 2.3$ ms, $\tau_2 = 22\ \mu s$, and $\tau_3 = 16.5\ \mu s$. The fitted value of $E_2'$ was subsequently confirmed to within experimental error ($E_{2_{obs}}' = 0.6 \pm .1$ meV) by direct spectroscopic observation, using the bulk excitation provided by the GaAs laser diode array.

Determination of the radiative lifetimes by this method, in conjunction with measurements of the absorption coefficient, allows one to make a reasonable estimate of the concentration of these isoelectronic centres, a measurement which had previously not been possible for the other IBE in Si due to their very low concentrations and oscillator strengths. In contrast, the Si:Be material shows strong absorption both at the no-phonon A line and at a series of narrow line excited states (Fig. 3.2b). The latter lines showed monotonically decreasing absorption strengths as a function of increasing energy, qualitatively similar to the hydrogenic s-like excited states previously reported in IBE in GaP:N.[36] For the Si:Be system however, the line spacings do not appear to fit into a Balmer type series, although they converge at an energy of approximately 40 meV, which can be taken as the approximate binding energy of the more weakly bound particle in the complex. The first and second of these lines are weakly observed in the high temperature luminescence spectra (Fig. 3.2c) confirming that they are in fact excited states. These data were obtained

with the absorption measurement technique outlined on page 10. All measurements were obtained with loosely mounted 3 mm thick samples of the previously described material, immersed in superfluid He.

Further structure was observed in the vicinity of the second and third excited states by means of excitation spectroscopy using the experimental system described in chapter 2. The luminescence intensity was monitored at the wavelength of the broad acoustic phonon replica B'(AC), which was conveniently removed from any of the no-phonon transitions. The nature of these subsidiary peaks has not been established.

Absorption was not observed for the less allowed B and B' transitions as expected, considering the lower oscillator strengths of these transitions. The lack of observed absorption for the $A_1, B_1, B_1'$ lines was indicative of the lower concentration of these binding centres as reflected by their much lower luminescence intensities relative to those of the A,B,B' lines ($I_1/I \sim 10^{-3}$).

The concentrations were calculated after the method of Dexter [37], which is based on the fundamental connection between the spontaneous emission and absorption rates, as expressed by the relationship between the Einstein A and B coefficients. The spontaneous emission rate of the A line is given by the experimentally observed A line decay rate, $\tau_3$. The strength of the transition is then expressed in terms of an oscillator strength, $f_A$, proportional to $1/\tau_3$:

$$f_A = \frac{m^* \; c \; \lambda^2 \; g_i}{8 \; \pi^2 \; e^2 \; n \; \tau_3 \; g_f} \qquad (4)$$

where $\lambda_A$ is the A line wavelength of $1.15 \times 10^{-4}$ cm, n = 3.5 is the

index of refraction, and $g_i$ and $g_f$ are the exciton and crystal ground state degeneracies of 3 and 1 respectively. Substituting an effective mass $m^* = 0.48m_o$ equal to the geometric mean of the longitudinal and transverse electron masses, appropriate for an isoelectronic donor (weakly bound electron), one arrives at an oscillator strength of $f_A = 1.54 \times 10^{-3}$. This represents the total oscillator strength of the A line and all of its phonon replicas. The concentration of optically active centres, N, is then related to the measured absorption profile $\mu(v)$ (in $cm^{-3}$) and the oscillator strength $f_A$ by :

$$Nf_A = \frac{nm^*c}{2\pi^2 e\hbar} \int \mu_A(E)\,dE \qquad (5)$$

A more convenient expression[37], which assumes a Gaussian line profile with linewidth $\Gamma$ (in meV) and peak absorption coefficient $\mu$, is given by:

$$Nf_A = (6.27 \times 10^{14}\ cm^{-3})\ \mu\Gamma \qquad (6)$$

Substitution of the experimentally obtained values of $u = 21.6\ cm^{-1}$ and the no-phonon A line absorption linewidth at half maximum, 0.65 meV, implies a concentration of $1 \times 10^{16}\ cm^{-3}$. This value includes a correction for the extra absorption due to the phonon replicas of the A line. From the luminescence spectra of Henry et al.[17], these replicas increase the total integrated absorption coefficient by a factor of approximately two. This high value of N is comparable to that observed earlier in compound semiconductors, such as GaP:Bi and ZnTe:O[11], and is consistent with the hypothesis of Crouch et al.[33] that the bulk of the Be dissolved in Si is

in the form of electrically inactive neutral Be-Be pairs.

Si:Li Results

Canham et al.[18] have reported spectral measurements on an intense band of lines observed in samples of electron irradiated Si:Li, characterized by a no-phonon triplet of lines near 1045 meV, and a complex set of lower energy phonon replicas. Their isotope doping studies appear to indicate the involvement of four Li atoms, based on energy shifts in the elaborate series of phonon replicas. As in the case of the Si:Be centres, a relatively high concentration of binding centres was indicated by the observation of absorption. The thermalization of the main no-phonon lines, labelled $Q_L$, Q, and R was studied as a function of temperature and appeared to follow the same behaviour as the no-phonon triplet in Si:Be. The $Q_L$ line is attributed to the dipole forbidden ground state transition (B' in Si:Be), and the Q and R lines correspond to the more allowed excited states (B and A in Si:Be). Fig. 3.4 shows spectral measurements on these lines undertaken in this project at the representative temperatures of 2.0, 4.2 and 15 K. The samples used in these measurements were supplied by Dr. Lightowlers and were prepared by a previously described diffusion technique followed by irradiation with 2 Mev electrons.[18] Apart from quantitative differences in the relative oscillator strengths, there is a great deal of similarity with the Si:Be results of Fig. 3.2.

Lifetime data obtained as part of this project confirm the isoelectronic nature of this luminescence system. Fig. 3.5 gives a summary of decay time measurements made in the range 1.2 K to 70 K. The low

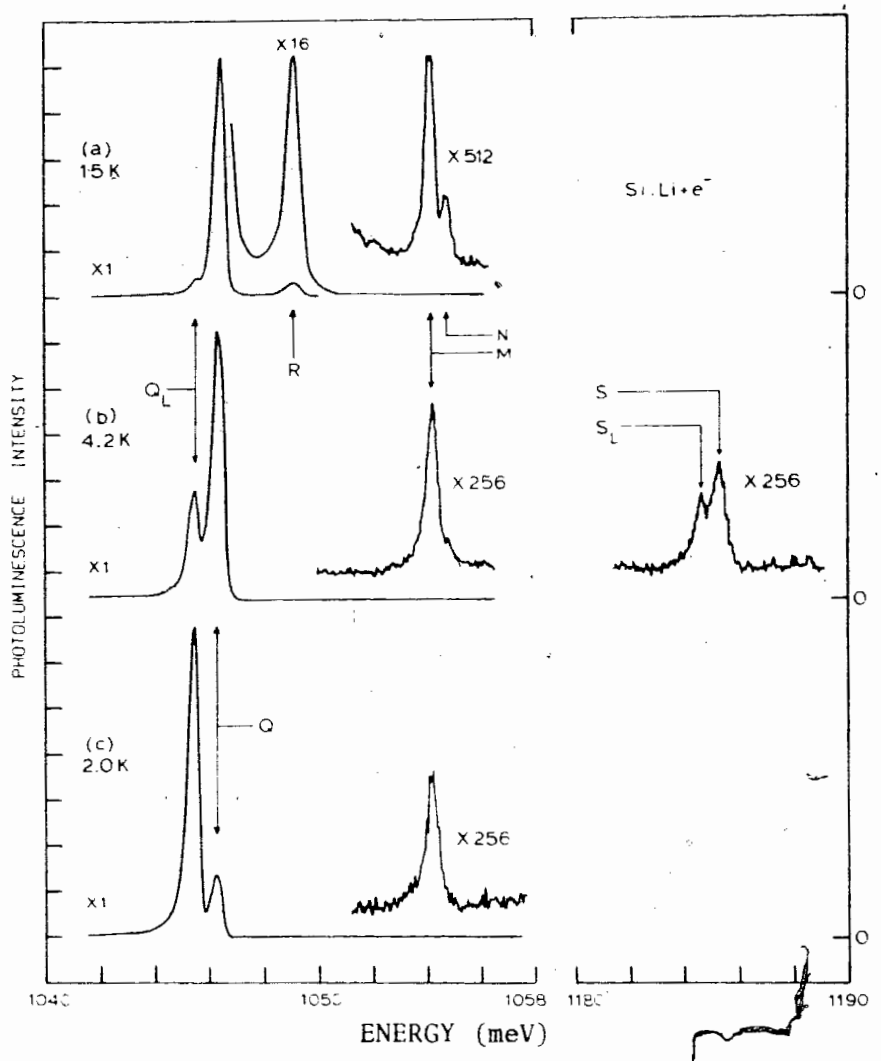


Fig. 3.4

Luminescence spectra for the three Si:Li IBE at various temperatures. The main set of lines Q, $Q_L$ are very similar to those of Si:Be. The intermediate energy lines, N, M have long lifetimes but do not show the same thermalizing triplet behaviour as the first set. The higher energy lines S, $S_L$ were too weak to observe at 15K and 2K in the samples used here.

temperature limit of 4 ms is the longest lifetime ever reported in Si. The decay times show the characteristic behaviour of the j-j coupling model as a function of temperature. A short plateau in the decay time at 15 K corresponds to the maximal thermal occupation of the allowed upper levels. Beyond these temperatures thermal quenching of the luminescence is observed.

In addition to the strong no-phonon luminescence lines observed near 1045 meV, Canham et al. reported a hitherto unknown set of weaker lines $S_L$ and S, at energies near 1085 meV, with very similar thermalization behaviour to the stronger, lower energy lines, $Q_L$ and Q. In the samples studied as a part of this project, these lines were observed to be roughly $10^{-3}$ times less intense in total integrated intensity relative to the $Q_L$, Q, R lines, although according to the work of Lightowler's group[18] the relative ratio of the two luminescence systems is strongly dependent upon the exact heat treatment and annealing procedure used in sample preparation. The samples which they studied in their preliminary work had a much higher ratio of high energy to low energy lines. In Fig. 3.4 only the 4.2 K spectrum is displayed since signal levels were very weak at all other temperatures. Despite the low signal levels a weak transient spectrum was obtained at 4.2 K with the TN-1750 multichannel scaler, using the stronger $S_L$ line. The observed lifetime of 240 μs at 4.2 K was highly indicative of an isoelectronic defect, although signal levels were too weak to obtain a detailed transient analysis over a range of temperatures.

The similarities between the two sets of Si:Be and Si:Li+$e^-$ IBE lines are suggestive of similarities in the binding centre structures. Both of the main Si:Be and Si:Li luminescence systems have weaker, higher energy

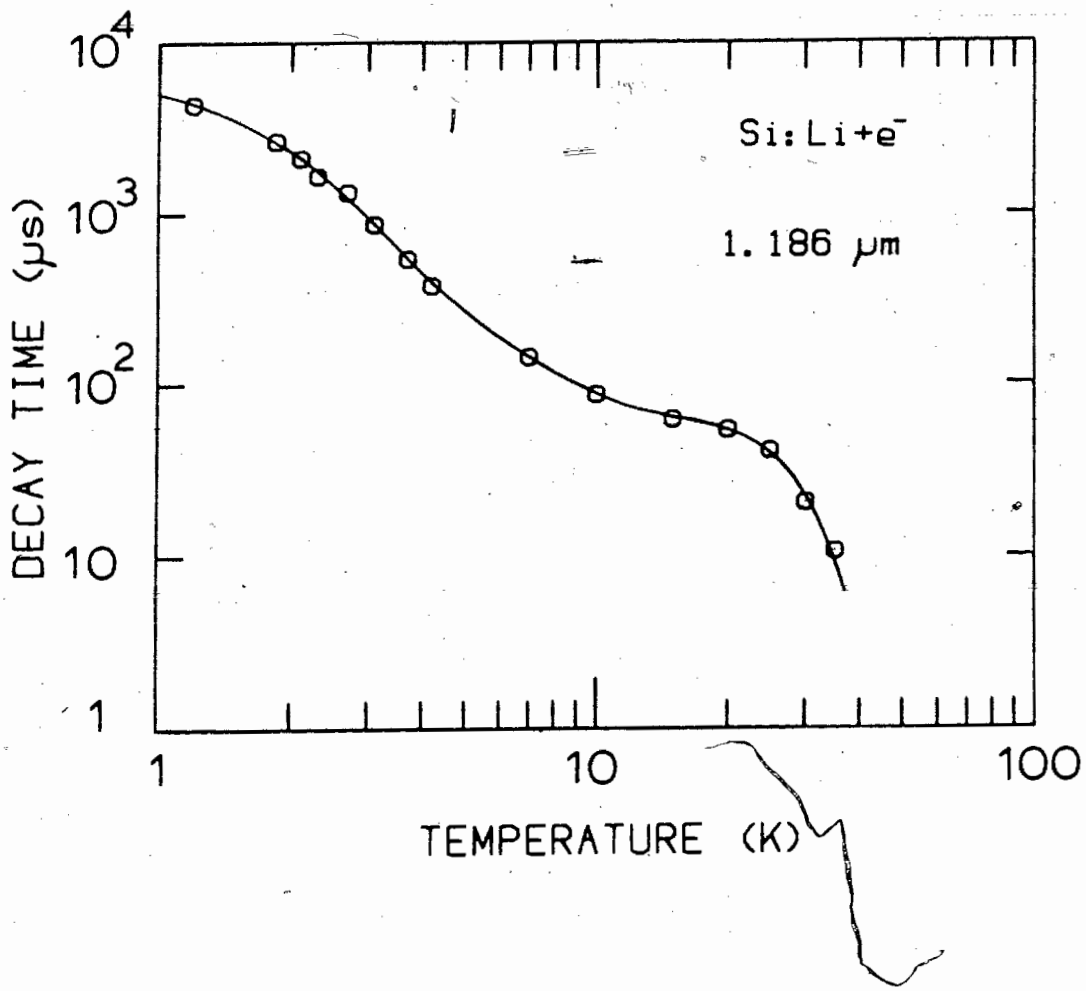


Fig. 3.5

Luminescence lifetime data for the 1045 meV (1.186 μm) Si:Li centre. The limiting low temperature lifetime occurs at 4.2 ms. The solid line is not a theoretical fit.

IBE lines roughly $10^{-3}$ times lower in intensity than the principal IBE centres. The ratio of the separations of the no-phonon lines of each pair of luminescence systems from the total energy gap of Si are 0.62 and 0.68 for Si:Be and Si:Li respectively. These two features suggest similarities with characteristics of the X-centre acceptors frequently observed in conjunction with normal substitutional acceptors in Si. For every group III acceptor in Si, there has been observed, in certain samples, a shallower acceptor level with concentrations in the range of $10^{-2}$ - $10^{-4}$ times that of the associated group III acceptor, and a binding energy ratio relative to that acceptor of $\sim 0.84$ to 0.73.[38] Jones et al.[38] have performed a detailed experimental study of the properties of the X-centres associated with each of the group III acceptors. They report experimental and theoretical evidence for a model in which X-centres arise as a result of the lowering of the central cell potential of the substitutional acceptor due to the presence of nearest neighbour C. The preliminary evidence based on the results of this project is therefore consistent with a model in which the central cell potential of the IBE binding centre is lowered by the presence of nearest neighbour C. For the case of Si:Be, Henry et al.[17] have concluded from the strong coupling of the dipole forbidden B' line to the continuum of acoustic phonons (B'(AC)), that the binding centre is an isoelectronic donor, i.e. the hole is tightly bound in a short range potential which would be reduced by the presence of nearest neighbour C. In the case of the Si:Li centres, there is no evidence of coupling to such low energy acoustic lattice phonons, however there is considerable coupling to a very broad vibronic band of undetermined origin.

The weak set of lines labelled M and N in Fig. 3.4 were not reported by Canham et al. and do not show the thermalization behaviour of the other two sets of lines. The N line is clearly an excited state, but there is no evidence of a lower lying dipole forbidden ground state equivalent to $O_L$ or $S_L$. Nevertheless, the measured lifetime of 60 μs appears to indicate an isoelectronic centre, although it is probably unrelated to the other two Si:Li centres, given the fact that Canham et al. have not reported any annealing dependence.

## IV. Si:Cu Results

Copper has long been known to introduce very deep levels into the bandgap of Si.[39] Its high diffusivity and solubility therefore make it a very undesirable contaminant in device technology.

The data presented in this chapter are based on spectral and lifetime measurements on a series of intense long-lived photoluminescence lines observed in samples of Cu-doped Si, with decay times as long as 670 μs at 13 K. These lines, which were first reported by Minaev et al.[40] and subsequently by Weber and Wagner[41], have have an elaborate local mode structure similar to that observed previously in isoelectronic binding centres in other semiconductors.

All photoluminescence measurements were made using samples of ultra high purity float zone refined Si. Five nines ( 99.999% ) purity Cu was deposited onto 1 mm thick wafers of Si by vacuum evaporation and driven in by diffusion in an Ar atmosphere using a silica tube furnace. Strong luminescence was observed after a drive-in interval of five minutes at 1100 C followed by a rapid thermal quench from 1100 C to room temperature in a 50:50 ethanol-water mixture. This quenching technique had been observed to produce dramatic enhancements of the IBE intensities in Si:Tl and Si:In samples.[22,23] While the nature of the mechanism responsible for the quenching enhancement is not understood in the prior cases, in Si:Cu the quenching is thought to prevent the precipitation of Cu as the sample cools.[42] Lengthening the drive-in interval produced no discernible enhancement of the luminescence, in agreement with the very high

diffusivity of Cu in Si at these temperatures.

Transient excitation was achieved by mechanically chopping the output of the $Ar^+$ laser. Sample heating was negligible as confirmed by the insensitivity of the measured lifetime to peak pump powers from 2 to 20 $W/cm^2$. Luminescence spectra were recorded with the previously mentioned Ge detector system as well as with the InGaAsP phototube. The rapid fall in the photomultiplier response in this spectral region was corrected by normalizing the data against the spectral output of a blackbody source, in this case a tungsten-halogen lamp.

A peculiar feature of the Si:Cu luminescence was the saturation of the luminescence intensity with a cw pump power of roughly 0.8 $W/cm^2$, indicating a very low concentration of binding centres.

A complete 4.2 K luminescence spectrum obtained with the Ge detector is shown in Fig. 4.1. The main no-phonon lines and their relevant phonon replicas are tabulated in Table 4.1. Using the previously mentioned blackbody source, it was verified that none of the structure was due to atmospheric absorption . The 1014.7 meV peak, labelled 0 is clearly a no-phonon line, having a considerably narrower linewidth than the lower energy lines. The lines observed at 7.0, 14.1, and 21.1 meV below the 0 line and labelled 1, 2, and 3 are associated with the excitation of one, two, and three 7.0 meV local mode phonon replicas respectively. Two less intense lines, denoted 0' and 0", appear as small shoulders on lines 1 and 2 at energies of 16.4 and 25.1 meV below the no-phonon line respectively. These lines are characterized as phonon replicas of the 0 line, involving the participation of local mode phonons with energies of 16.4 and 25.1 meV respectively. In addition, weak lines are also observed at energies of 7.0

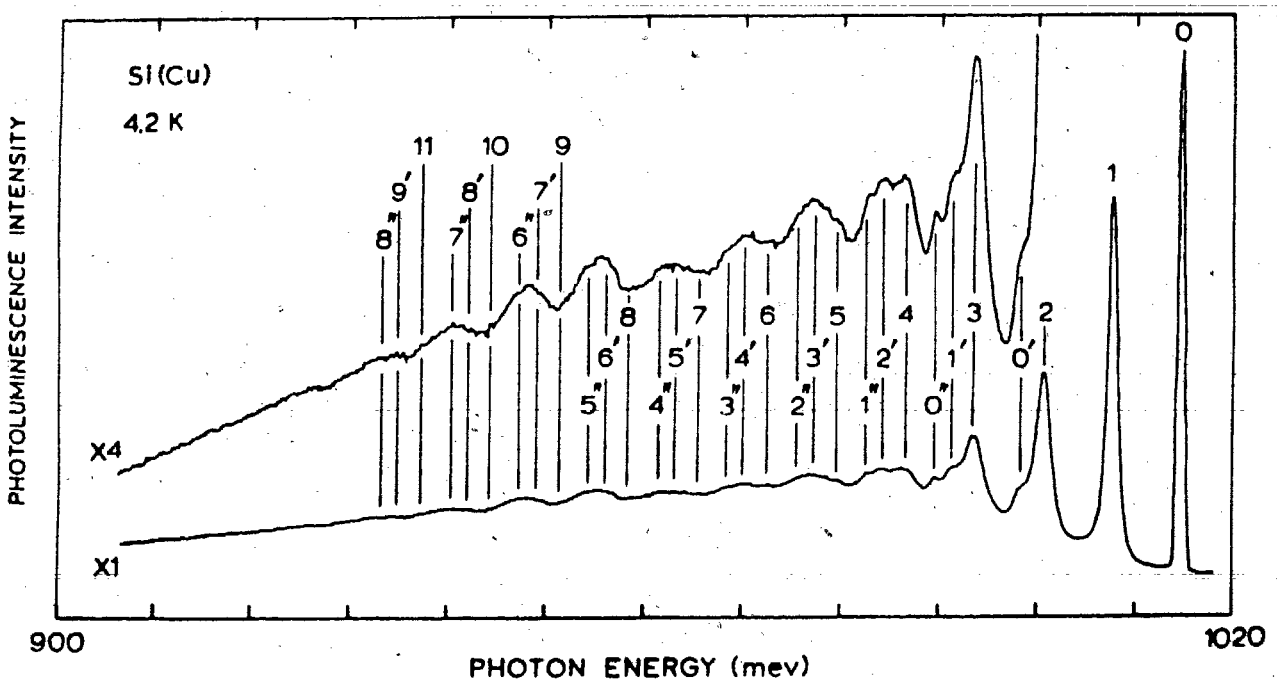


Fig. 4.1

Photoluminescence spectrum of Si:Cu measured at 4.2K with an intrinsic Ge detector. Lines 0 through 11 are ascribed to a no-phonon ground state and its 7.0 meV local mode replicas. The primed and double primed series correspond respectively to the excitation of single 16.4 and 25.1 meV phonons plus an integral number of 7.0 meV phonons. These data have not been corrected for detector response.

and 14.1 meV below the 0' line, and at 7.1 meV below the 0" line. These are labelled 1', 2' and 1" respectively and are attributed to the replication of the 0' and 0" lines through multiple excitation of one ( lines 1' and 1" ) or two ( line 2' ) 7.0 meV phonons.

On the basis of the identifications made above, line positions were calculated for three series of lines. The first series, labelled 0, 1,..., m is characterized by the excitation of zero, one, and up to m 7.0 meV phonons. The second series, labelled 0', 1',..., m' is characterized by the excitation of one 16.4 meV phonon together with zero, one or m 7.0 meV and the third series, labelled 0", 1",..., m by the excitation of one 25.1 meV phonon together with zero, one, or m 7.0 meV phonons. The calculated line positions shown in Fig. 4.1 by vertical lines were obtained by subtracting integral multiples of 7.0 meV from the energy of the primary line of each series (0, 0', 0"). No line positions for multiple 16.4 or 25.1 meV phonons are shown.

Beyond the fifth main peak ( consisting of components 4, 2' and 1" ) in the observed spectrum, the broadening becomes so great that contributions from the individual modes cannot be resolved. Note that the photoluminescence intensity shifts from the 0, 1, 2 ... series to the 0', 1', 2' ... and 0", 1", 2" ... series as the number of 7.0 meV phonons participating in the transition increases. Beyond the sixth main peak, which consists of components 5, 3' and 2", the primed and double-primed series dominate in intensity. The result is that the centroid of the nth envelope is gradually displaced further and further to lower energies from the energy defined by $E_{NP} - nE_{ph}$ as n increases, where $E_{NP}$ is the no-phonon transition energy and $E_{ph}$ is the energy of the primary 7.0 meV

Table 4.1

Line Energies for Si:Cu Centre

| Line | Energy (meV) | Displacement from Main NP line (meV) |
|---|---|---|
| 0 | 1014.7 ± .2 | |
| 1 | 1007.7 ± .3 | 7.0 |
| 2 | 1000.6 ± .3 | 14.1 |
| 3 | 993.6 ± .4 | 21.1 |
| 0' | 998.3 ± .5 | 16.4 |
| 1' | 991.3 ± .3 | 23.4 |
| 2' | 984.2 ± .4 | 30.5 |
| 0" | 989.6 ± .3 | 25.1 |
| 1" | 982.5 ± .5 | 32.2 |
| -1 | 1021.4 ± .5 | 6.7 |
| -2 | 1028.4 ± .5 | 13.7 |
| -3 | 1041.4 ± .5 | 20.3 |
| 0* | 1016.6 ± .2 | 1.9 |
| 0** | 1024.2 ± .2 | 9.5 |
| ? | 1015.7 ± .3 | 1.0 |

local mode phonon.

This local mode structure is quite similar to that observed in Cd-doped GaP by Morgan et al.[43] and by Henry and Dean.[44] Morgan et al. reported a set of lines in GaP:Cd which they ascribed to a no-phonon IBE transition with local mode replicas corresponding to phonons with 7.4, 9.0 and 37.0 meV energies. From oxygen isotope doping studies it was confirmed that the centre consisted of a nearest neighbour Cd acceptor - O donor pair. The 7.4 meV local mode converted each primary transition into a series of up to twelve lines. At low temperatures, a weak dipole forbidden ground state transition was observed on the low energy side of the main no-phonon transition indicative of j-j coupling of the electron and hole. As can be seen in the temperature dependent photoluminescence data presented in Fig. 4.2, no such weakly allowed ground state is observed for the Si:Cu system. These data were obtained with the photomultiplier system and therefore corrections for detector response were applied. All relevant line energies from both the photomultiplier and the Ge data are presented in Table 4.1.

At 35 K, two thermally populated excited state transitions $0^*$ and $0^{**}$ were observed at 1016.6 and 1024.3 meV respectively. The sharpness of these lines indicates that they correspond to no-phonon transitions of electronic excited states of the centre. In addition, three broad lines -1, -2, and -3 appear at 6.7 $\pm$ 0.5, 13.7 $\pm$ 0.5 and 20.3 $\pm$ 0.5 meV above the 0 transition. These are interpreted as anti-Stokes phonon replicas of the 0 line corresponding to the annihilation respectively, of one, two and three thermally excited 7 meV local mode phonons in the initial state. As the temperature was increased further to 50 K, some structure remained,

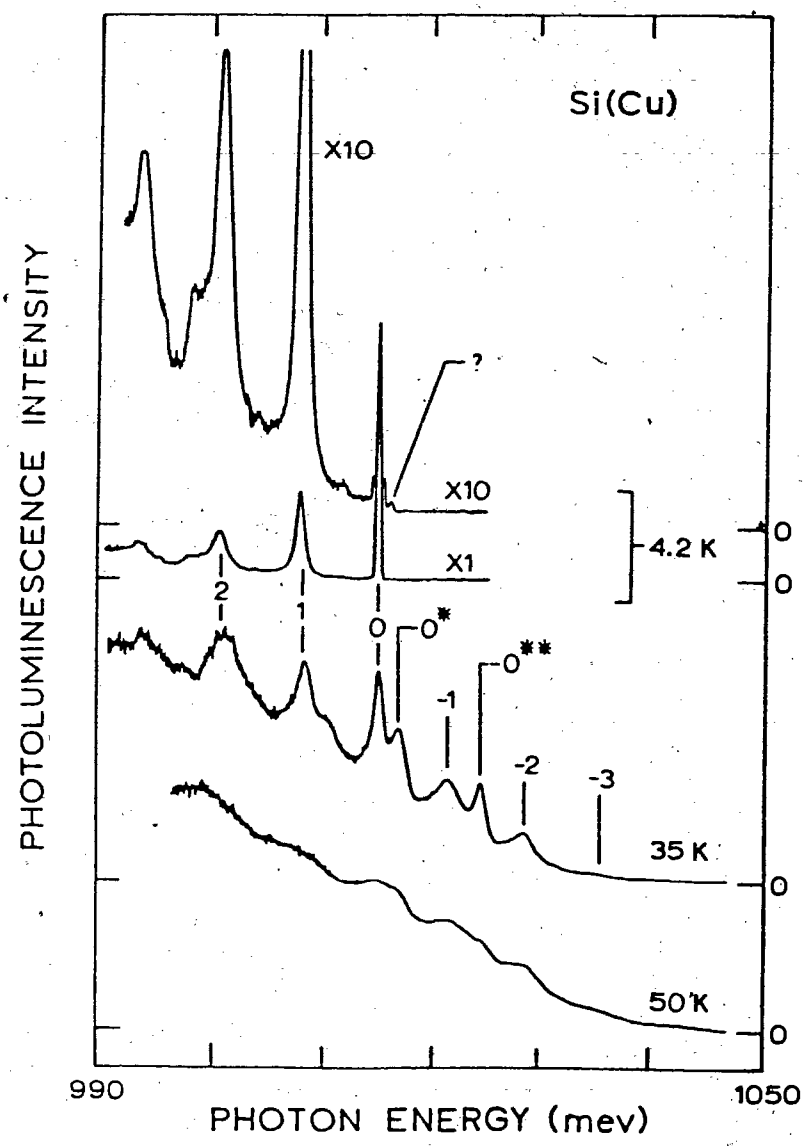


Fig. 4.2

Photoluminescence spectra measured at the representative temperatures of 4.2K, 35K, and 50K with the photomultiplier system. At higher temperatures, two excited states, $0^*$ and $0^{**}$ are evident as well as broad anti-Stokes replicas -1, -2, and -3 corresponding to a 7 meV local mode of the initial state. Data have been corrected for detector response.

although the broad band background increased markedly. Beyond 50 K, the entire spectrum merged into a featureless broad band.

At 4.2 K the photomultiplier data indicated a very weak, narrow line labelled ? in Fig. 4.2 at an energy 1 meV above that of the principal no-phonon transition. Since this line was not observed at 1.3 K, it may be due to another electronic excited state of the centre.

Fig. 4.3 gives decay time data taken for the intense no-phonon line, O, over the temperature interval from 1.3 to 50 K. Lifetime measurements for the phonon replica lines 1 and 2 were in good agreement with this data, which confirms that all lines originate from the same binding centre. The very long decay times observed, ranging from 480 μs at 1.3 K to 670 μs at 13 K, clearly point to some form of isoelectronic binding centre.

The possibility of a dipole forbidden ground state lying below that responsible for the O line is excluded on the basis of this transient data, since this would result in a marked increase in the lifetime with decreasing temperature, as was observed in the Si:Be systems. The decrease in lifetime below 4.2 K suggests that there may be a longer lived excited state very near the ground state transition.

Since the decay time continues to decrease with decreasing temperatures even below 2 K, at which point all of the observed electronic excited states ( ?, $O^*$ and $O^{**}$ ) are depopulated, these data suggest that there is another very low-lying excited state which has not been resolved in our spectra.

The rapidly decreasing lifetime above 20 K may result from thermal breakup of the binding centres, but a small shoulder at 50 K could indicate that the falling lifetime above 20K is partially due to the

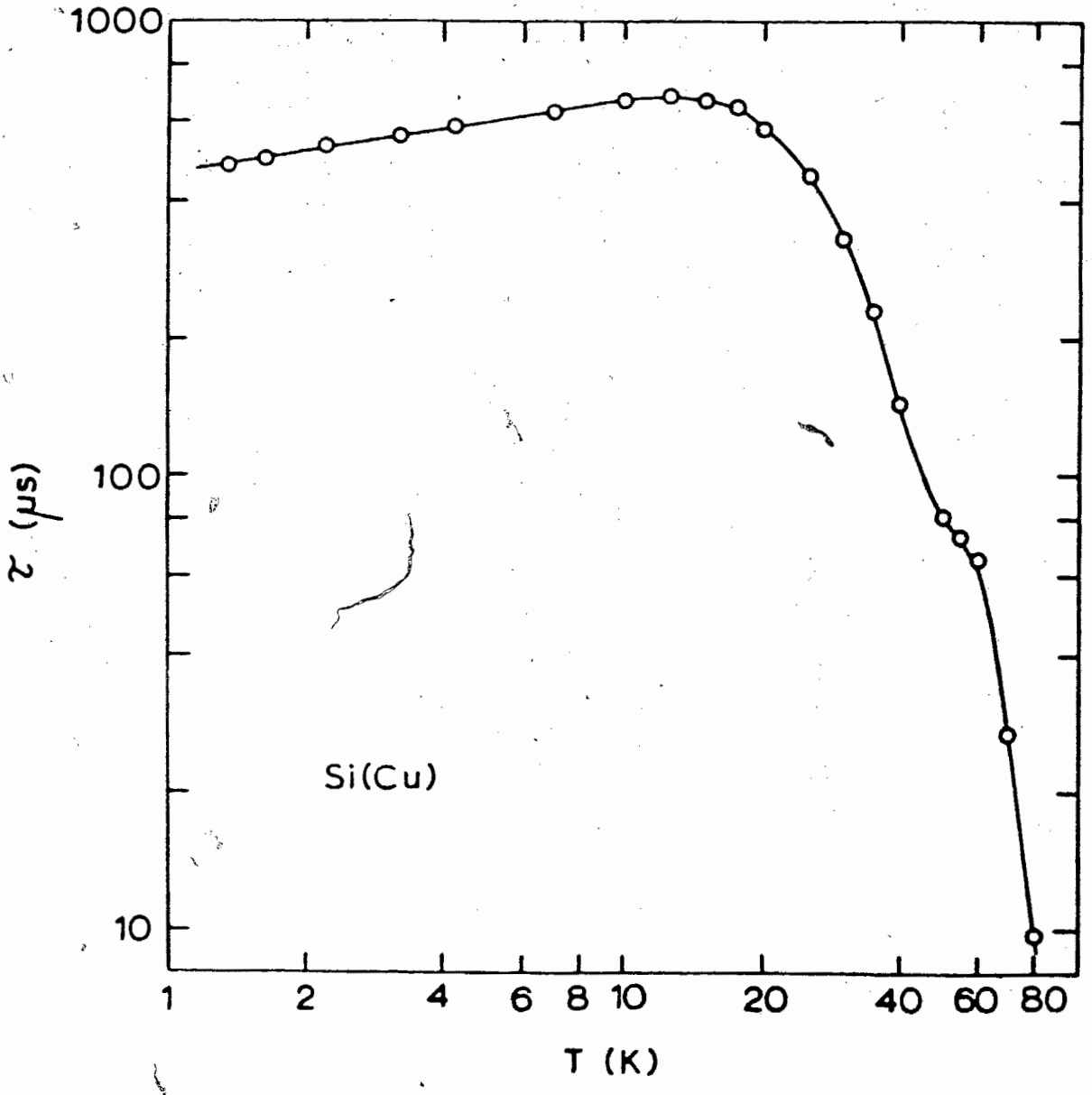


Fig. 4.3

Experimental decay times of the main no-phonon Si:Cu line (0) as a function of temperature.

thermal population of shorter lived excited states such as $O^*$ or $O^{**}$. Such behaviour is familiar form the Si:Be data, as well as from many other "typical" isoelectronic centres.

The strong couplings to local mode and acoustic lattice phonons observed in this centre are suggestive of a large degree of lattice relaxation. In the HTL model, the first bound particle is very tightly bound in the short range central cell potential of the isoelectronic impurity. The capture of this particle therefore causes a certain amount of relaxation of the surrounding lattice due to the large concentration of charge near the defect. The weakly bound second particle, with its more extended wave function, should not affect this local relaxation. Since the equilibrium displacements of the defect and lattice ions may be considerably different, a number of local mode or lattice phonons may be excited on recombination of the exciton. Such a model is usually described in terms of a configuration coordinate diagram in which the total elastic + electronic energy of the defect + lattice is plotted against some relative lattice coordinate (see Fig. 4.4). In the adiabatic and Frank-Condon approximations, the relative strengths of the phonon replicas is simply given by the degree of overlap of the initial and final vibrational wave functions, whose equilibrium coordinates are off-set by some displacement $q_0$. The relative intensities of the phonon satellites are then given by a simple Poisson distribution

$$I\ (h\omega_o + nh\omega_q) = e^{-S_q} \left(\frac{S^n}{n!}\right) \qquad (1)$$

where $S_q$ represents the relaxation of the ground state for the vertical

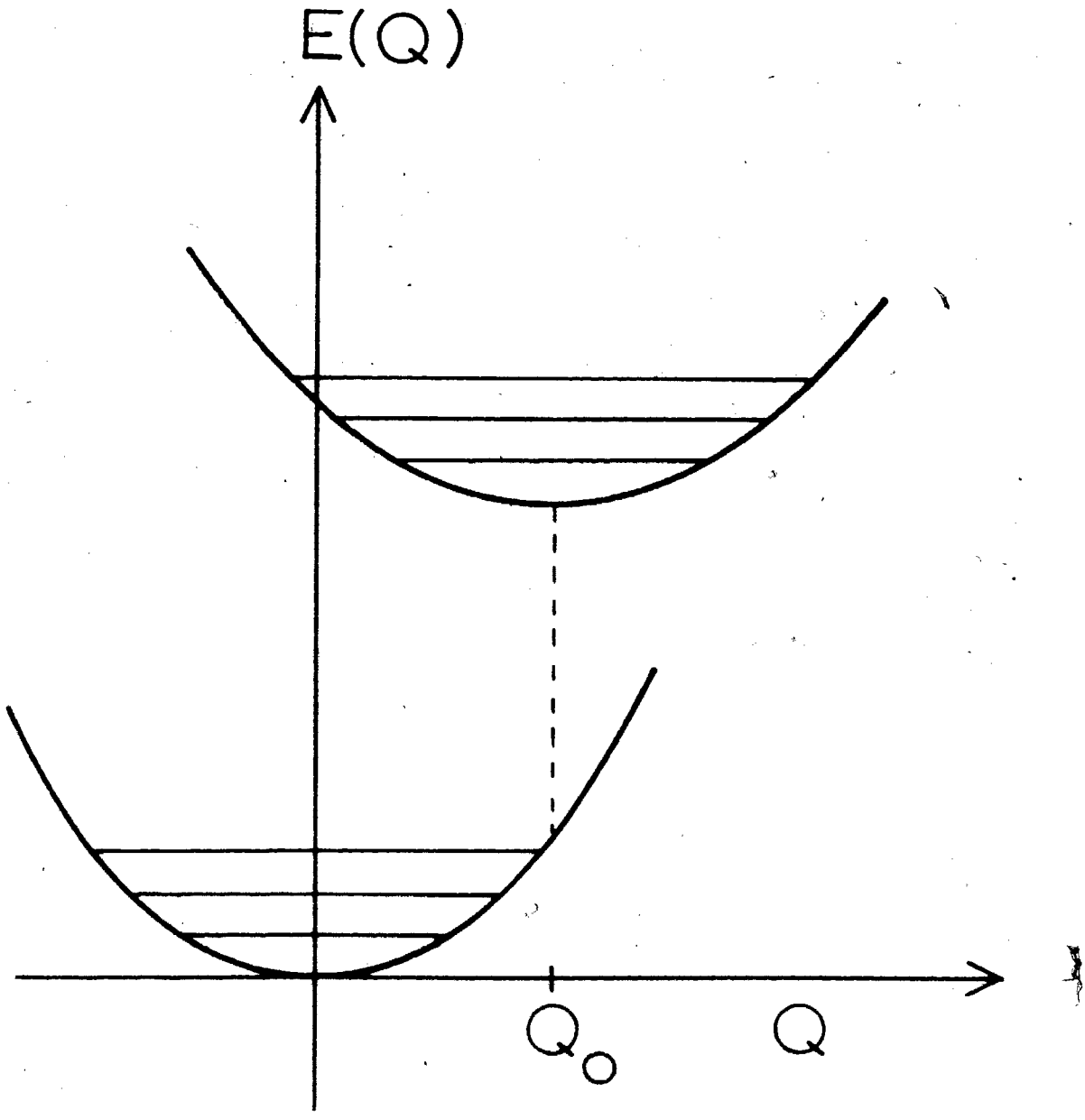


Fig: 4.4

Configuration coordinate diagram for a centre such as Si:Cu in which the exciton and the crystal ground state couple to the same lattice coordinate, but with different equilibrium positions. Recombination of the exciton is accompanied by the emission of several local mode or lattice phonons.

transition shown in units of the ground state phonon energies, $E_q = h\omega_q$. $S_q$ can be viewed as the average number of phonons emitted in the above relaxation process. The total electron phonon coupling strength for a given centre is stated as a sum of the $S_q$ factors for each mode. This is given by the ratio of the no-phonon integrated line strength to that of all of the phonon replicas. For the case of Si:Cu the low temperature value of $S_{tot}$ is given by $S_{tot} \sim 3$, which is relatively low compared to the values reported in more ionic semiconductors.

Recent measurements by Weber et al.[32] on the Si:Cu system indicate a very large discrepancy between the thermal dissociation energy and the spectroscopically determined binding energy of the exciton. Their data is consistent with a very large binding energy of 155 meV for the tightly bound particle (35 meV for the weakly bound), adding further evidence of relatively large lattice relaxation. This is consistent with the above lattice relaxation model.

## V. Acceptor Related Results: Si:Tl and Si:In

### Experimental Results

The group III acceptors In and Tl are known to introduce very deep acceptor levels into Si at respectively 157 mev and 246 meV above the valence band edge.[5,45] Acceptor bound exciton luminescence has been observed at energies well below the free exciton edge from both of these acceptors.[19] Both systems show the rapid decay times on the order of nanoseconds expected for the Auger dominated decay of a bound exciton.[12,13] In contrast, the isoelectronic lines associated with Si:In and Si:Tl have decay times of approximately 200 and 25 - 50 μs respectively.[20,22,24]

The measurements undertaken in this study were obtained with a variety of samples obtained from different sources. Samples from two different boules of Czokralski grown Si:In with nominal concentrations of $4 \times 10^{15}$ In $cm^{-3}$ (Si:In 24) and $5 \times 10^{17}$ In $cm^{-3}$ (Si:In 23) were used, as well as samples derived from a boule of float zone refined material with a concentration of approximately $2 \times 10^{16}$ In $cm^{-3}$ (Si:In 112). For the Si:Tl measurements, two different samples were used, one with a concentration of $5 \times 10^{16}$ Tl $cm^{-3}$ (Si:Tl 21) and the other with a much lower doping level of $4 \times 10^{14}$ Tl $cm^{-3}$ (Si:Tl 25). All samples were subjected to the same quenching procedure, which involved heating them to between 900 and 1100°C, and dropping them into a 50:50 mixture of ethanol

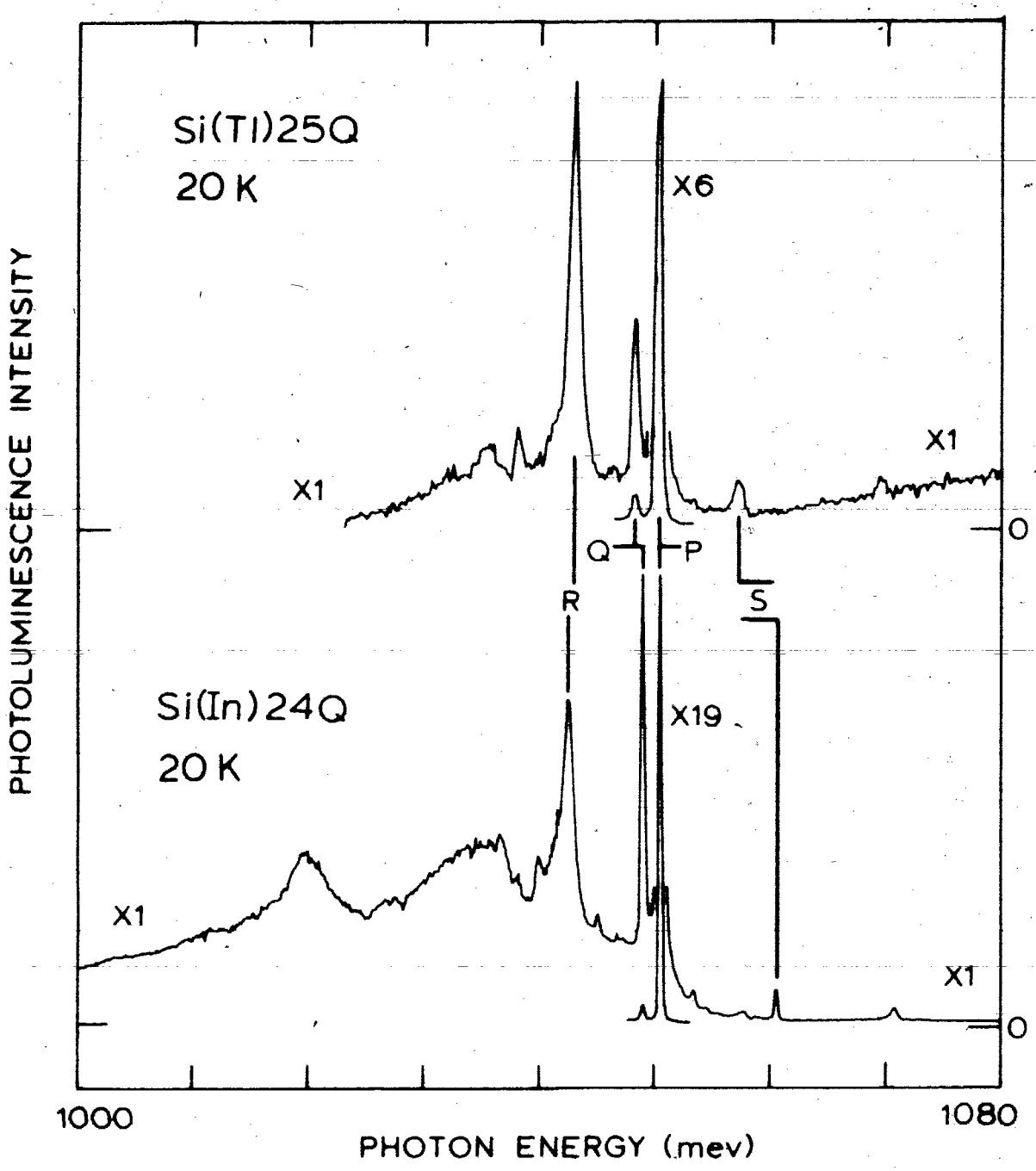


Fig. 5.1

A comparison of the 20K Si:Tl luminescence system with the P,Q,R luminescence system in Si:In at the same temperature. The Si:In spectrum has been shifted down in energy by 67.4 meV to align the principal no-phonon P transitions (from Thewalt et al.[24]).

and water. This quenching treatment leads to enhancements in the Si:In luminescence intensity by factors of up to $10^3$.[22] The addition of ethanol results in a lower quench rate as compared to 100% $H_2O$, and a subsequently lower concentration of binding centres, but produces less risk of sample fragmentation.

Continuous excitation was achieved with either the $Ar^+$ or the $Kr^+$ ion lasers, while pulsed excitation was provided either by electro-optical modulation of the $Kr^+$ laser, or more predominantly by means of the GaAs laser diode array, which was capable of producing much shorter pulses ($\Delta t \sim 300$ ns)

The 20 K spectral data is summarized in Fig. 5.1 from Thewalt et al.[24], in which the Si:In P,Q,R luminescence system is shifted down in energy by 67.4 meV to align the predominant no-phonon P line with that of the Si:Tl system in order to show the remarkable similarities in the spectral features. Both systems of lines are characterized by the sharp no-phonon line labelled P, as well as sharp line excited states Q and S. The designation of Q as due to an excited initial state is based on the thermal activation of its intensity relative to P, and implies that the final state corresponds to an excited state of the bare binding centre, probably a local mode phonon excitation. The broad feature labelled R shows no activation relative to P for both Si:Tl and Si:In, and is therefore designated as an exciton ground state to bare binding centre excited state transition . In addition, for the case of Si:In, broad featureless bands labelled * and ** are observed, and have been attributed by Stahlbush and Forman [27] to coupling of the ground state transition to the regions of high densities of states in the Si lattice phonon spectrum, due to the

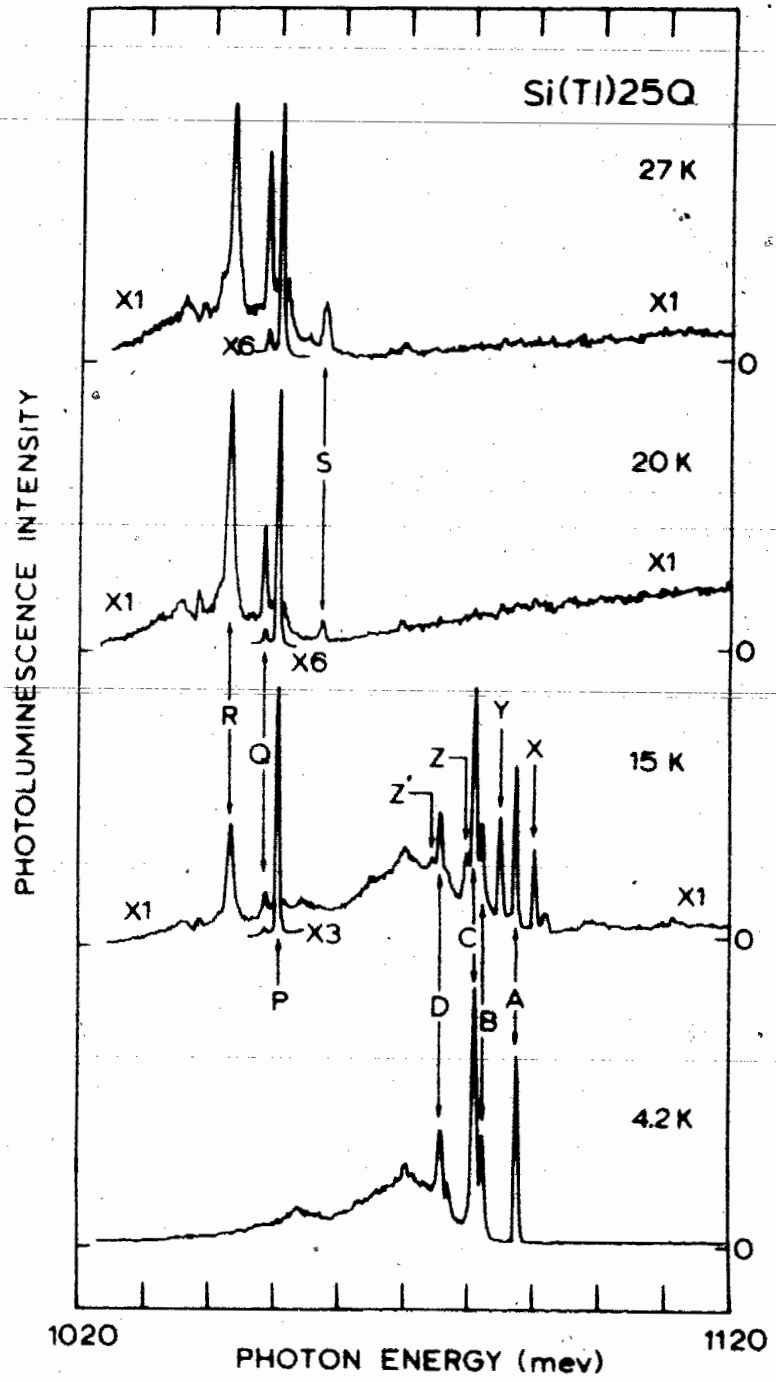


Fig 5.2

Spectra of Si:Tl 25 ($4X10^{14}$ Tl $cm^{-3}$) taken at 4.2K, 15K, 20K, and 27K, showing the drastic changeover in the luminescence features. This changeover was completely reversible (from Thewalt et al.[24]).

drastic breakdown of momentum conservation rules. Thewalt et al.[26] have proposed that, since the 67.4 meV energy separation of the Si:Tl and Si:In P lines is a large fraction of the 91 meV difference between the Tl and In acceptor binding energies, both excitons are isoelectronic donors, i.e. the hole is primarily bound by the deep central cell potential of the acceptor impurity, with the electron more weakly bound in the resulting long range Coulomb potential.

Whereas the Si:In P,O,R luminescence does not change significantly in cooling below 20 K, the Si:Tl P,O,R luminescence vanishes for temperatures below 12 K and is replaced by a completely new set of lines, A,B,C, for which the ground state to ground state transition, or A line, lies 36.8 meV above the P line. The temperature dependence of the changeover is shown in Fig. 5.2 from Thewalt et al.[24], based on measurements of the lightly doped Si:Tl 25 sample.

Detailed thermal activation measurements, due to Thewalt et al.[24], have resulted in the proposed energy level scheme of Fig. 5.3, in which excitation of local modes of the bare binding centre appears to account for most of the structure. The relative magnitude of the no-phonon transition to the total phonon replica oscillator strengths is shown in Fig. 5.4. These data were obtained with the same Ge dectector system used for the spectral measurements of Fig. 4.4 and do not suffer the drastic cutoff in detector response of the photomultiplier tube. The Si:Tl spectrum shows considerably stronger coupling to a broad band of phonon replicas than does the Si:In data. The integrated intensity of all Si:Tl lines does not change appreciably in passing through the transition, indicating that the total number of excitons responsible for both sets of lines remains a constant.

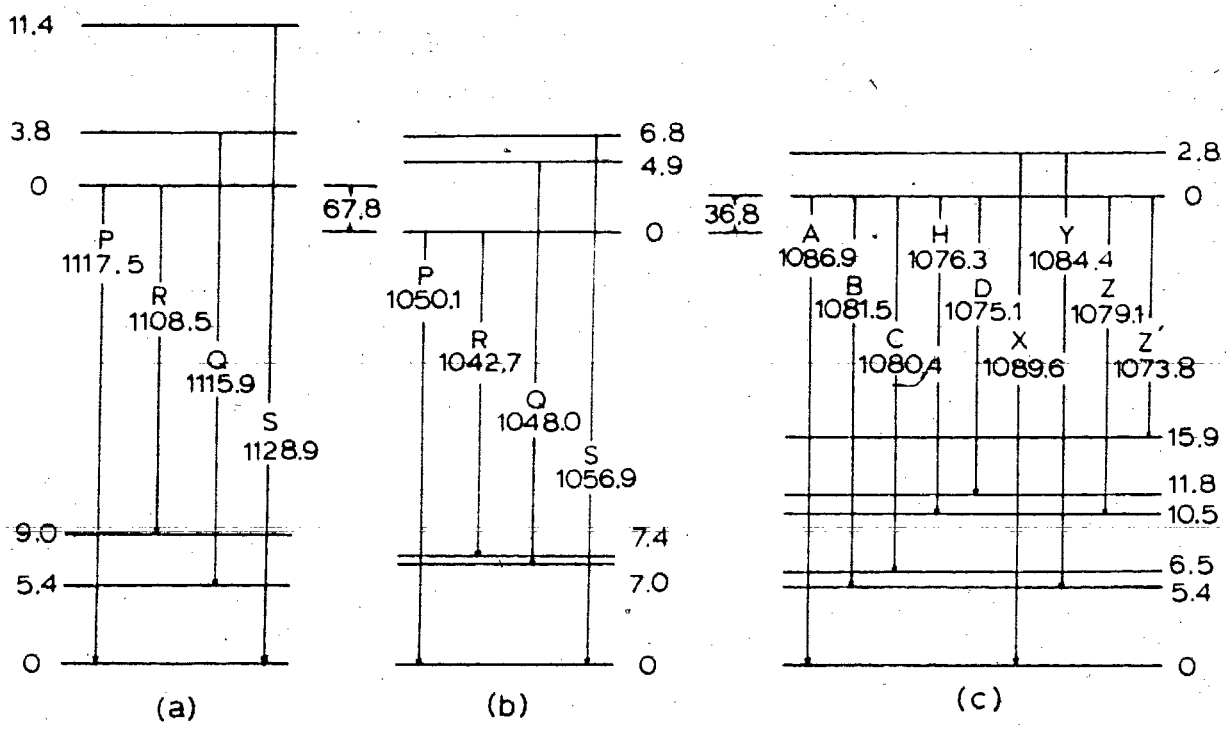


Fig. 5.3

(a) and (b) show the energy level spacings of the strongest lines in the P,Q,R systems in Si:In and Si:Tl respectively (from Thewalt et al.[24]). All energies are in meV. The upper lines represent IBE levels while the lower lines correspond to various excitations of the bare binding centre. (c) shows the completely different structure of the Si:Tl A,B,C luminescence system, in which the bare centre couples to various local mode phonons.

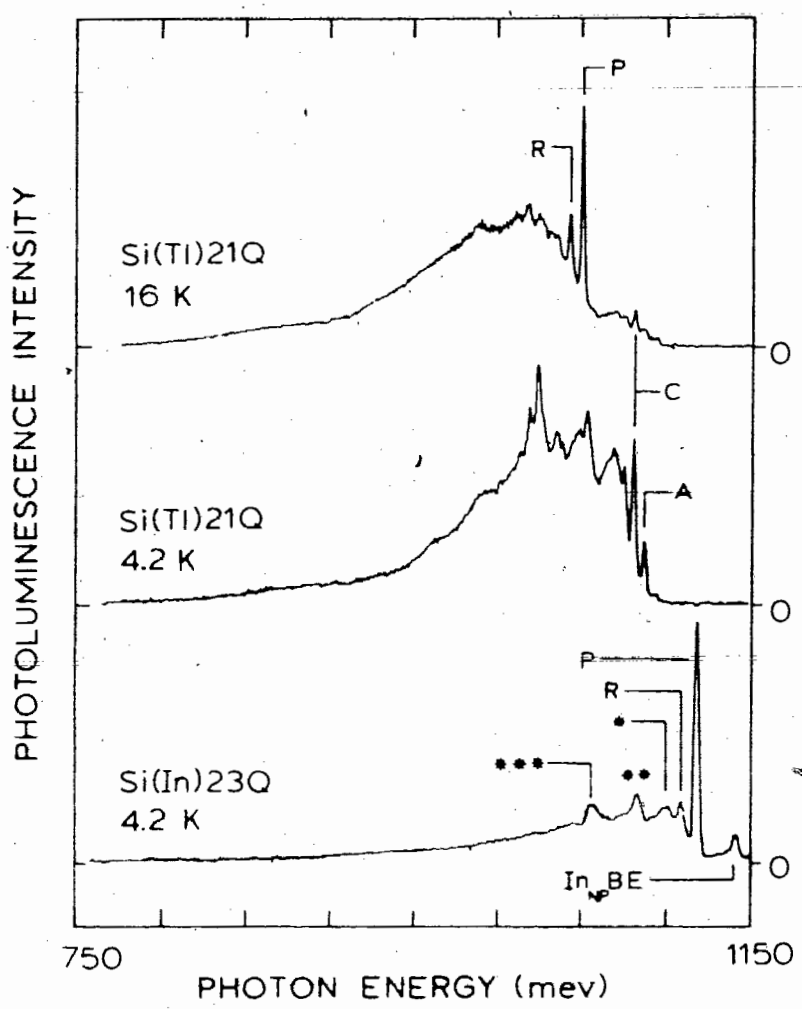


Fig. 5.4

Spectra of Si:Tl at 4.2 and 16K and of Si:In at 4.2K obtained with the intrinsic Ge detector( from Thewalt et al.[24]). The Si:Tl centre shows very strong coupling to a broad band of phonon replicas at both temperatures. The phonon band from the A,B,C system causes strong spectral interference with the Si:Tl P,Q,R system between 12 and 14K. The phonon coupling for Si:In is considerably less than for Si:Tl in agreement with its much shallower central cell potential.

This unusual changeover was found to be completely reversible and, based on the results of two widely differing samples, material independent.

## Si:Tl Transient Results

The main clues as to the nature of the Si:Tl changeover process are to be found in the novel transient behaviour of this system. All transient measurements on these samples were obtained with the GaAs laser diode array, which provided the required short pulses as well as good bulk excitation of the samples, due to the longer wavelength (870 nm). Using the previously described quenching technique, average luminescence signal levels of up to $10^4$ photon counts per second second were obtained, using a laser pulse repetitionrate in the vicinity of 2 kHz.

The transient behaviour of all the A,B,C related lines and the related phonon replicas was found to be identical. Similarly all P,Q,R related lines showed the same transient behaviour, which differed drastically from that of the A,B,C related lines. These observations offer evidence that the two sets of luminescence lines originate from two distinct isoelectronic binding centres which will be denoted simply by A or P. The A-centre transient data is summarized in Figs. 5.5 and 5.11, with the numerical values given in Table 5.1. The A-centre decay curves were accurately exponential over several decades with a constant decay time of 53 μs at temperatures between 1.2 K and 10 K. For this temperature range, good counting statistics (up to 4 decades of linearity) were obtained with a collection time of approximately 15 minutes. Concurrent with the rapid

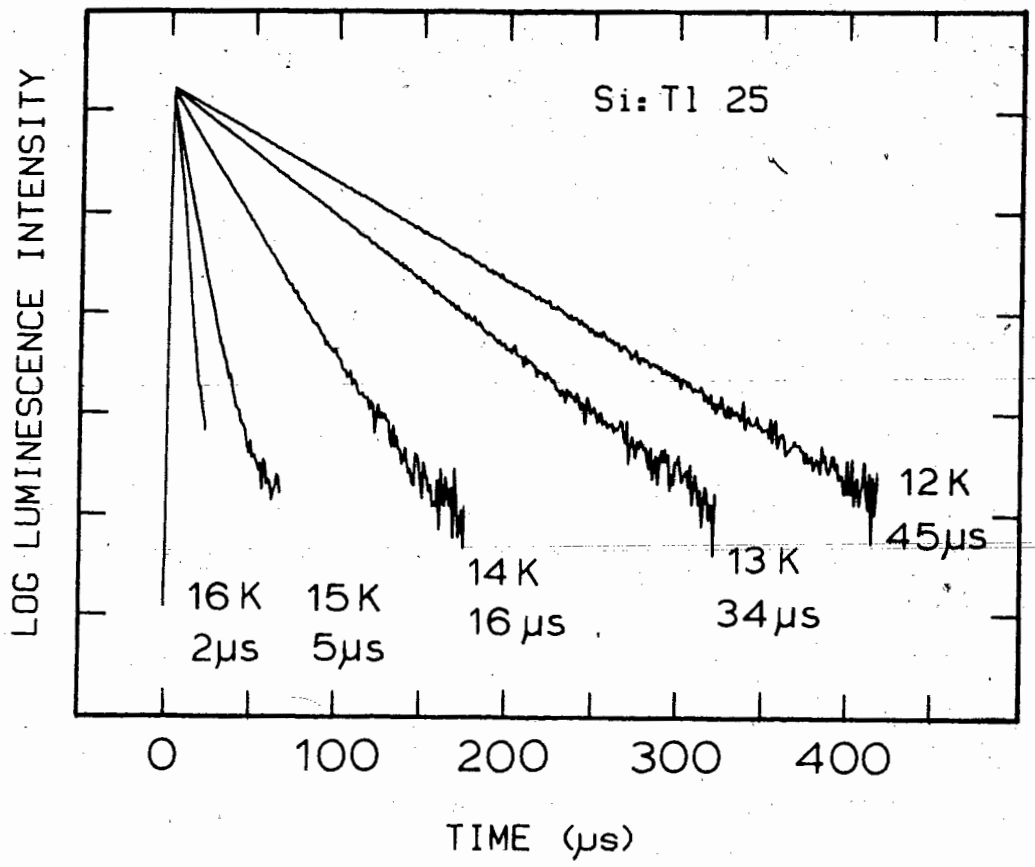


Fig. 5.5

Transient luminescence curves for the A-centres in Si:Tl at representative temperatures, measured using the strong C-line. All curves share the same baseline, indicating that the initial concentration of A-centres is independent of temperature. Vertical axis markers are decades.

drop in A,B,C line intensity above 10 K was a rapid decrease in the A-centre lifetime. Very weak A-centre luminescence was observed up to 20 K, at which temperature the time-to-amplitude converter indicated a lifetime of approximately 500 ns. Since the data presented in Fig. 5.5 share the same baseline, the fact that the initial luminescence intensity is essentially temperature independent indicates that both the exciton capture cross-section and initial concentration of A-centres are also temperature independent.

The transient behaviour of the P-centres, as summarized in Figs. 5.6, offers the most revealing insight into the nature of the changeover process. At the intermediate A-P changeover temperatures (12-18 K), and immediately following the laser excitation pulse, a relatively slow buildup of the luminescence was observed, followed by the subsequent standard exponential decay. Fig 5.7 shows a linear plot of the buildup at 14 K, at which temperature the luminescence intensity reaches its peak 20 μs after the excitation pulse. Measurement of the true P line intensity was complicated at temperatures below 14 K by spectral interference from the broad band of phonon replicas of the A-centre (see Fig. 5.4). A background transient spectrum was obtained by accumulating signal at wavelengths on either side of the P line for a time equal to that of the P line measurement. For the 12 K and 13 K data, the background subtracted P line transient spectra had a much more pronounced buildup. Above temperatures of approximately 18 K, the buildup became so rapid that the measured P line transient spectra were essentially exponential over several decades, with a constant decay time of 25 μs up to temperatures of 30 K, beyond which thermal quenching drastically increased the decay rate. All of these

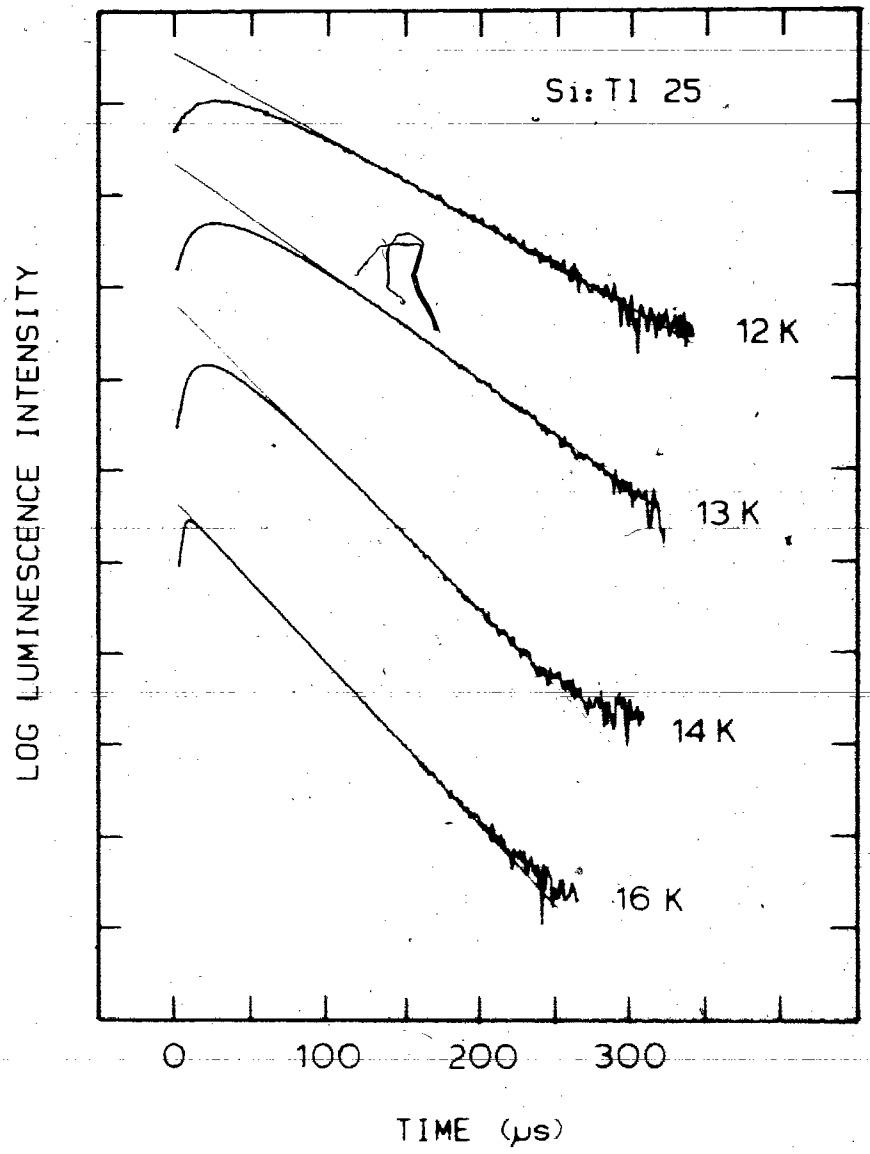


Fig. 5.6

Transient luminescence curves for the P-centres in Si:Tl at representative temperatures, showing the considerable buildup in luminescence intensity after the laser pulse. Above 16K the buildup becomes extremely rapid and the luminescence effectively decays with a single exponential. The baselines have been offset to contrast the buildup behaviour. The straight lines represent least squares fits to the long time portion of the decay curves. Data were collected using the strong no-phonon P line. Vertical axis markers are decades.

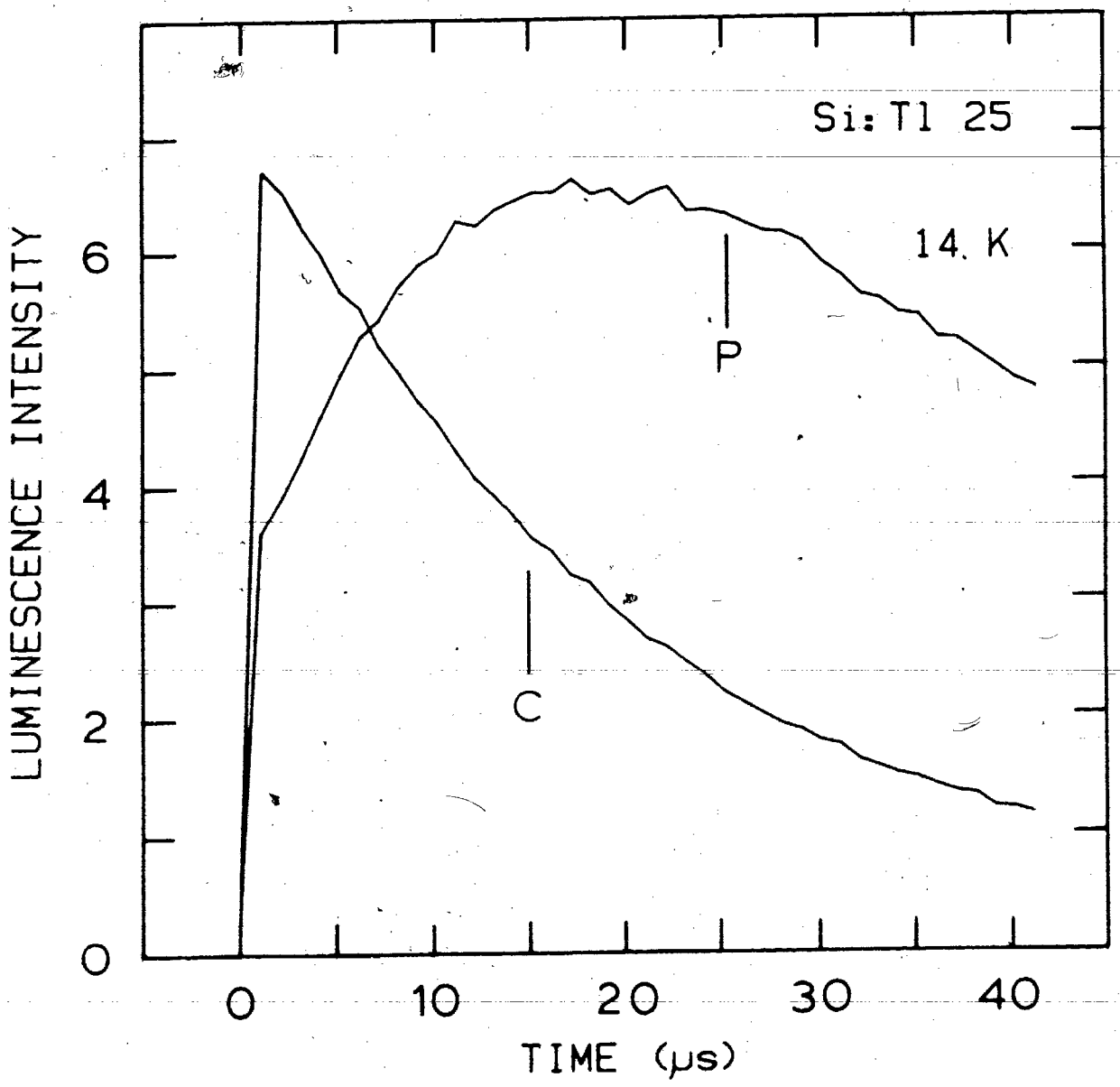


Fig. 5.7

Transient spectra of the P and A-centres measured separately at 14K. The data are displayed on a linear scale in order to show the full magnitude of the buildup. The P-centre intensity is seen to rise from some non-zero value at t=0.

results were found to be independent of both the pump repetition rate and the peak pump intensity. The pump repetition rate was varied from the optimum value of 2 kHz to 100 Hz with no discernible difference in the decay spectra. Similarly no difference was observed after the pump intensity was reduced by factors of 10 and 100 by means of neutral density filters.

The above data are readily explained in terms of a model in which the buildup of P,Q,R luminescence is due to the thermally activated transformation of A-type IBE into P-type IBE.[24] In such a model, excitons would be bound to a binding centre which could exist in one of two configurations, A or P. Excitons initially bound in the A configuration would be prevented at low temperatures from converting to the more energetically favourable P configuration by the presence of some energy barrier, $E_B$. At higher temperatures, thermal activation of the changeover rate would account for the buildup of P,Q,R luminescence and a decrease in the integrated A,B,C luminescence. Assuming that the energy of the P exciton ground state was substantially lower than that of the A exciton, at high temperatures the A line luminescence would vanish completely as the changeover rate became exponentially large.

These considerations are indicated schematically in Fig. 5.8 in which $E_X$ and $E_G$ represent the displacement of the P-centre exciton ground state and bare binding centre ground states respectively. The spectroscopically observed difference between the no-phonon A line and P line place the constraint that $E_X + E_G = 36.8$ meV.

The simplest possible set of rate equations describing the above model is:

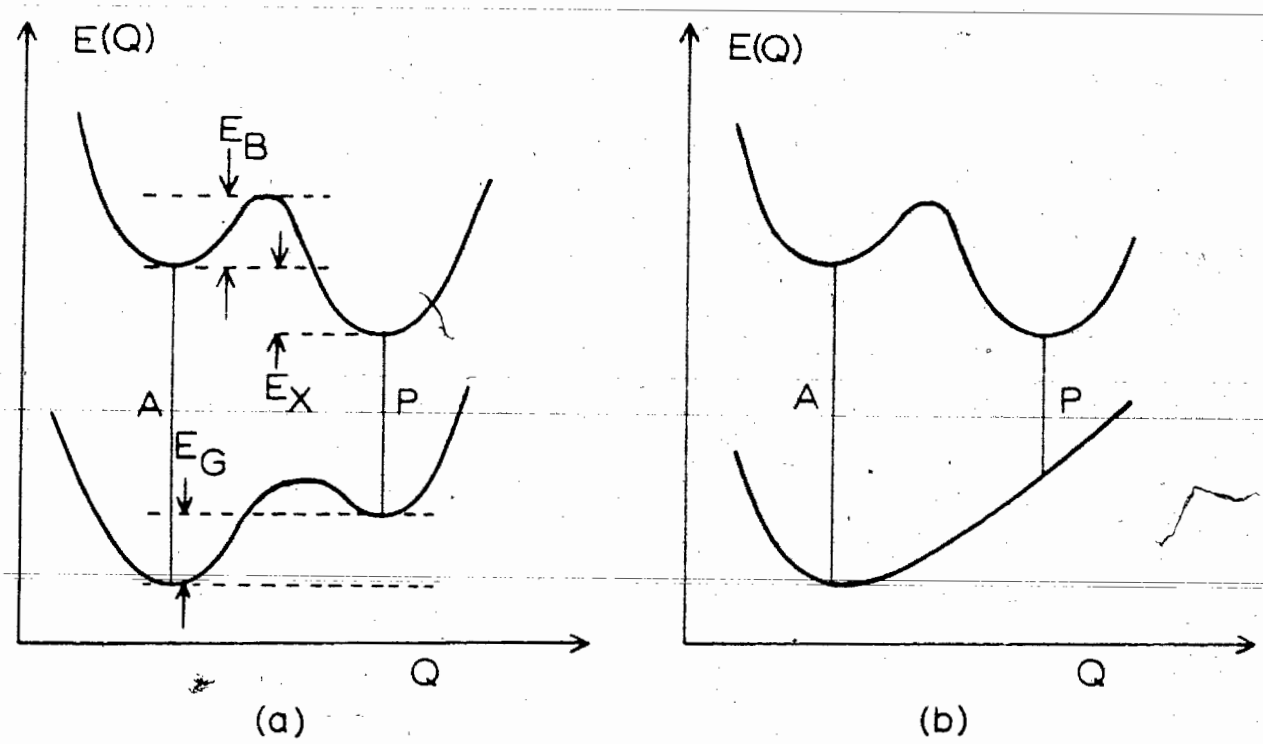


Fig. 5.8

(a) and (b) represent two possible configuration coordinate diagrams for the Si:Tl centre. In both cases excitons are created predominantly in the A configuration, and can then convert into P-type excitons by thermally overcoming the energy barrier $E_B$. If $E_X$ is large enough, there can be no feedthrough back to the A-type configuration. In (a), however, the bare binding centre has a metastable excited state which can be thermally populated at sufficient temperatures.

$$\frac{dn_A}{dt} = -\frac{n_A}{\tau_A} - \frac{n_A}{\tau_{AP}} \tag{1}$$

$$\frac{dn_P}{dt} = -\frac{n_P}{\tau_P} + \frac{n_A}{\tau_{AP}} \tag{2}$$

where $n_A$ and $n_P$ are the populations of the A and P-centres, $1/\tau_P$, and $1/\tau_A$ are the respective radiative decay rates, and $1/\tau_{AP}$ is the rate of feedthrough from A to P. Assuming initial IBE populations $N_A$ and $N_B$ gives:

$$n_A(t) = N_A\, e^{-t/\tau_A'} \qquad \left(\frac{1}{\tau_A'} = \frac{1}{\tau_A} + \frac{1}{\tau_{AP}}\right) \tag{3}$$

$$n_P(t) = N_P\, e^{-t/\tau_P} + \frac{\tau_P}{\tau_{AP}}\left(\frac{\tau_A'}{\tau_A' - \tau_P}\right) N_A(e^{-t/\tau'} - e^{-t/\tau_P}) \tag{4}$$

Hence, the condition for buildup to occur is:

$$N_P < N_A\left(\frac{\tau_A}{\tau_{AP}}\right)\left(\frac{\tau_A}{\tau_A - \tau_P}\right) \tag{5}$$

All of the above constants should be directly determined by the experimental data, requiring no adjustable parameters. The radiative decay time of the P-centre was determined from the T > 18 K P,O,R lifetime data for which the luminescence decays with essentially a single temperature independent exponential time constant of 25 μs (Table 5.1). The radiative decay time of the A-centre, as determined from the low temperature A,B,C measurements was 53 μs. The feedthrough time $\tau_{AP}$ is given by :

$$\tau_{AP} = \frac{(\tau_A - \tau_A')}{\tau_A \tau_A'} \tag{6}$$

Table 5.1

Si:Tl Transient Results

| T (K) | $\tau_A$ (μs) | $\tau_{P,L}$ (μs) | $\tau_{P,S}$ (μs) | $\tau_{AP}$ (μs) |
|---|---|---|---|---|
| 12 | 45 | 46 | 22 | 298 |
| 13 | 34 | 36 | 23 | 94.8 |
| 14 | 16 | 26 | 14 | 22.9 |
| 14.5 | 9.4 | 25 | | 11.4 |
| 15 | 5.3 | 25 | 5.9 | 5.9 |
| 15.5 | 3.4 | 25 | | 3.6 |
| 16 | 2.3 | 24 | 2.7 | 2.4 |
| 17 | 1.1 | 25 | | 1.1 |
| 20 | | 25 | | |
| 30 | | 23 | | |

$\tau_A$ is the observed lifetime of the A-related lines, which always decay as a single exponential. $\tau_{P,S}$ and $\tau_{P,L}$ are respectively the observed short exponential buildup time and long exponential decay time of the P-related lines. $\tau_{AP}$ is the calculated transfer time from A-centres to P-centres.

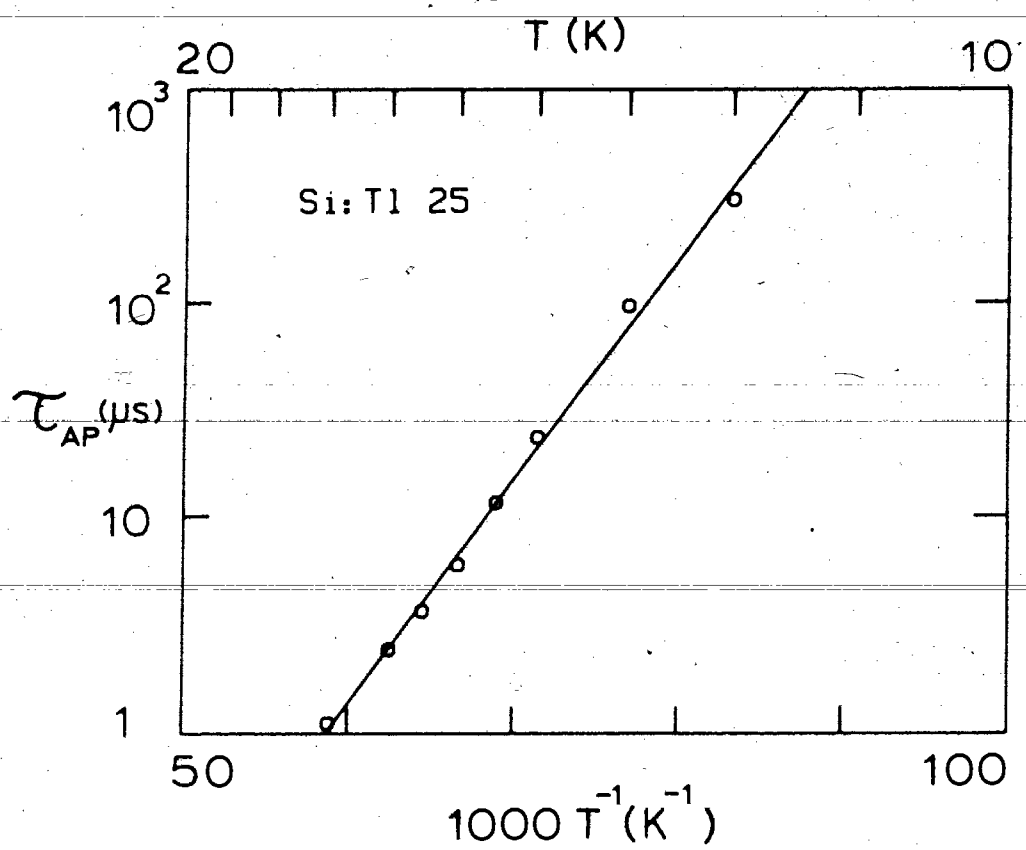


Fig. 5.9

The log of the feedthrough rate $\tau_{AP}$, as calculated from the experimental data using the model described in the text, plotted against 1/T. This rate shows an activation energy of 20.5 meV with a pre-exponential factor of 9 X $10^{-13}$, based on a least squares fit to the curve.

where $\tau_A'$ is the measured A-centre lifetime for $T < 18$ K. $\tau_{AP}$ is plotted in Fig. 5.9 on a log versus 1/T plot. A least squares fit to the data yields an exponential activation of the feedthrough time given by:

$$\tau_{AP} = \tau_o e^{E_B/kT} \tag{7}$$

with $E_B = 20.5$ meV and $\tau_o = 9 \times 10^{-13}$ s. This expression is consistent with thermal activation over a classical barrier of energy $E_B$. The small prefactor is indicative of a phonon mediated process.

The predictions of equation (4) are easily verifiable in terms of the experimental data. If condition (5) is assumed to hold, then the P line transient data should consist of the sum of two exponentials with prefactors of opposite sign and time constants $\tau_A'$ and $\tau_P$, where $\tau_A'$ is equal to the A-centre decay time. These predictions are confirmed by the results displayed in Fig. 5.10, which represent the result of subtracting the experimental P line decay data points of Fig. 5.6 from a simple exponential decay curve obtained from a least squares fit to the exponential part of the long time decay portion of the luminescence intensity (also shown in Fig. 5.6). In Fig. 5.10 the $t < 0$ points represent the long time fit while the $t > 0$ points correspond to the exponential responsible for the buildup portion. In all cases, the resultant spectra were linear over more than two decades. The labels $\tau_S$ and $\tau_L$ refer to the short and long time constants corresponding respectively to the buildup and long time decay times of the P line luminescence. Equation (4) implies that for the temperatures for which $\tau_A' < \tau_P$, the buildup time constant $\tau_S$ is given by $\tau_S = \tau_A'$, whereas

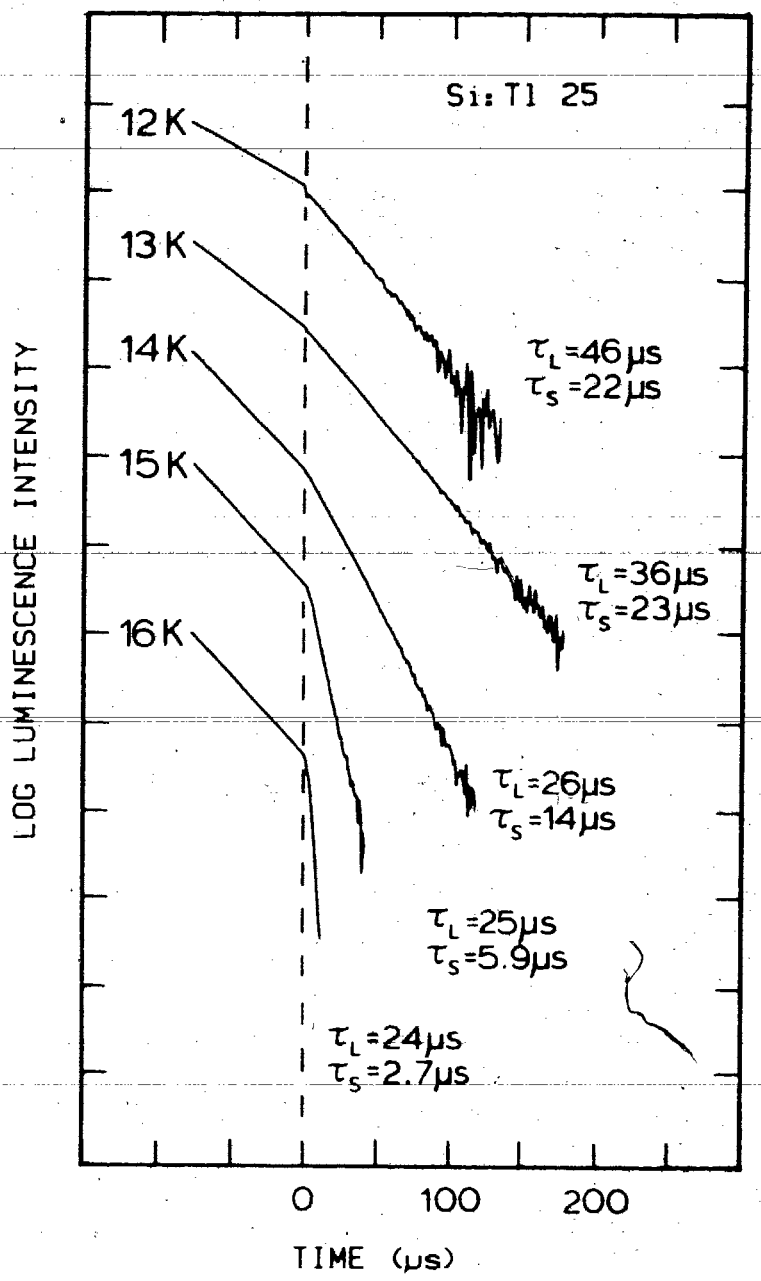


Fig. 5.10

These curves represent the result of subtracting the experimental P-centre data points shown in Fig. 5.6 from the least squares fits to the long time limits of the decay curves. These data clearly show the presence of two simple exponential contributions to the P-line transient curves. The lines shown at $t<0$ represent the fits to the long-time decay portion, while the steeper $t>0$ lines represent the exponential responsible for the buildup. Vertical axis markers are decades.

the long time constant $\tau_L$ is given by $\tau_L = \tau_P = 25\ \mu s$. For temperatures at which $\tau_A' > \tau_P = 25\ \mu s$, the roles are reversed and one has $\tau_S = 25\ \mu s$ and $\tau_L = \tau_A'$. These predictions are verified in Fig. 5.10 to within experimental uncertainty. The complete picture of the transient data is summarized in Fig. 5.11 over the temperature interval from 4 K to 35 K. The squares represent the observed A-centre decay time, $\tau_A'$ while the circles represent the time constants of the P-centre buildup, $\tau_S$. The crosses represent the fitted long time decay times of the P line, $\tau_L$, as determined from Fig. 5.6. As predicted by (4), $\tau_L$ maintains the constant value of 25 $\mu s$ up to the temperatures at which thermal dissociation of the binding centres occurs (T > 30K). For the temperatures for which $\tau_A' > \tau_P$ (i.e. T < 13.5 K), the measured values of $\tau_S$ deviate slightly from their expected values of 25 $\mu s$ due to the very low P line intensities at temperatures below 14 K. The presence of the previously mentioned spectral interference from the broad phonon replica bands of the A,B,C lines made background correction difficult at these temperatures. Since the decay time of the A-centres is in principle exactly equal to that of the long time constant $\tau_L$ at these temperatures, there is no other way of removing the background than the procedure described previously.

The curved solid line in Fig. 5.11 corresponds to a plot of $\tau_A'$ versus T with $\tau_A'$ given by :

$$\tau_A' = \frac{\tau_A \tau_{AP}}{\tau_A + \tau_{AP}} \qquad (8)$$

where the feedthrough rate $\tau_{AP}$ is given by (7). The intersection of this curve with the constant line at 25 $\mu s$ gives the temperature at which

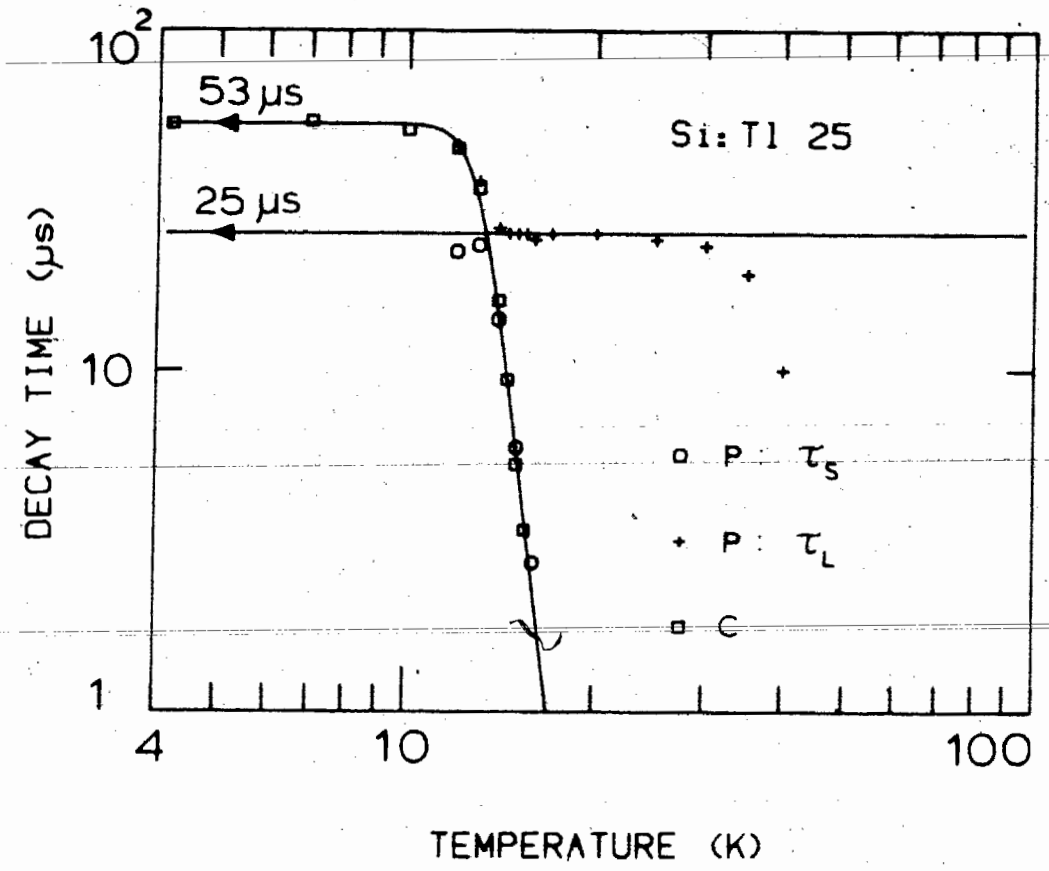


Fig. 5.11

Summary of the Si:Tl transient data. The squares represent the measured A-centre lifetimes. The circles and crosses represent respectively the short and long time constants of the P-centre transient luminescence results as derived in Fig. 5.10. The falling P-centre lifetime above 30K is due to thermal dissociation of the IBE.

$\tau_A' = \tau_P$, namely 13.5 K.

The above analysis has clearly demonstrated that the exciton can exist in one of two different binding centre configurations, and that a thermally activated changeover process can occur from a higher energy state, A, to a lower energy state, P, which is separated by an energy barrier of 20.5 meV. The results however offer no evidence as to whether the the bare binding centre can exist in one of two different configurations before the capture of an exciton (as depicted in Fig. 5.8a).

In an effort to resolve this question, several short time resolution runs were undertaken with the time-to-amplitude converter both during and immediately after the excitation pulse. The 14 K linear plot of the P line transient data shown in Fig. 5.7, obtained with the multichannel scaler, clearly indicates the presence of some initial t = 0 P-centre population, which appears in a time less than the instrumental resolution of even the subsequent time-to-amplitude converter measurements, unlike the following slow buildup. Such an initial concentration could be due either to the thermal population of the bare P-centre defect or to reconfiguration of the exciton and binding centre during the capture process. These two possibilities are indicated schematically in Fig. 5.6 by configuration coordinate diagrams. Fig. 5.8a corresponds to the existence of a metastable bare P-centre configuration. From the spectroscopic splitting of the A and P-centre no-phonon lines, and the lack of P-centre luminescence below 10 K, this metastable level must lie above the bare A-centre ground state. In Fig. 5.8b, the final state is not metastable but quickly relaxes back to the bare A-centre ground state. Measurements taken with the time-to-amplitude converter show the initial t = 0 population to be

thermally activated from approximately 14 K to 17 K with an activation energy of 4 meV, however above 18 K, the buildup time becomes too rapid to draw any conclusions regarding the initial population. Below 14 K the value of the initial intensity obtained depends strongly on the exact wavelengths used in the background subtraction. A 4 meV activation energy is inconsistent with the observed lack of any P line luminescence below 10 K. The possibility that an energy barrier may exist between the bare binding centres was investigated by looking for a pump power or repetition rate dependence, but as described previously, no effect was observed.

## Large Lattice Relaxation Model

The important role of lattice relaxation in radiative and non-radiative transitions in semiconductors has only begun to be recognized in the last decade. Langer[46] distinguishes between two conceptually different forms of lattice relaxation, for which evidence is available in both highly ionic and covalent semiconductors. The first, referred to here as type I, is associated with the concentration of electric charge induced by a deeply bound defect and the subsequent rearrangement of the defect after recombination (IBE or bound exciton recombination) or ionization (deeply bound hole or electron). This was proposed in chapter 4 as the explanation for the relatively strong phonon coupling in the case of Si:Cu, in which a very tightly bound particle ($E_B$ = 155 meV) was responsible for considerable lattice relaxation after recombination . This model also quantitatively accounts for the difference in the phonon coupling strengths between the two Si:Tl IBE and that of Si:In. From Thewalt et al.[24], the

thermal binding energy for the Si:In P,Q,R lines was found to be 36 meV, which was in agreement with the observed spectroscopic energy difference relative to a free exciton band edge of 36.8 meV, and was therefore interpreted as corresponding to the thermal dissociation of the exciton as a whole. The measured thermal binding energy of the Si:Tl P,Q,R lines was 47 meV. The difference between this and the measured spectroscopic energy difference with respect to the conduction band edge of 119.2 meV gave a hole binding energy of 72 meV, indicating that the hole is much more tightly bound for the case of Si:Tl. This fact is reflected in the total phonon coupling strengths as indicated in Fig. 5.4. Based on these data, the ratio of the integrated no-phonon intensity to the total integrated intensity of the phonon replicas imply Huang-Rhys factors of S = 4.4 and S = 8.1 for the P,Q,R luminescence systems of the Si:In and Si:Tl systems respectively. These S values correspond to relatively large electron-phonon couplings in comparison with other semiconductors.[47] The much larger phonon coupling strength of the A,B,C luminescence system ($S \sim 10^2$) is puzzling, considering that the no-phonon line wavelength is considerably shorter than that of the Si:Tl P line, a fact which would usually indicate a shallower binding centre.

The second form of lattice relaxation in Langer's classification corresponds to the hopping of the binding centre constituents between non-equivalent lattice sites, rather than a mere local stretching or contraction of the local impurity lattice bonds after a change in localization of one of the bound particles. A severe example might correspond to hopping of one of the binding centre constituents from a substitutional to an interstitial site. Well documented cases of such

phenomena were based on the observation of metastable donor levels in the highly covalent semiconductor InSb[48,49], as well as in the more ionic material CdTl:Cl.[50] Both of these systems were explained in terms of two different donor levels separated by a configurational energy barrier, $E_B$. Transient transport measurements yielded the very large respective barrier energies of 300 meV and 500 meV. The relaxation times associated with the low temperature limits in these cases exceed the limits of experimental observation ($t > 10^6$ hr).

The existence of double well configurations for lattice relaxation of type I is also well documented. Piekara et al.[51] used such a model to account for two metastable donor levels associated with highly ionic semiconductor CdF :In. In such materials, an electronic excited state can be accompanied by very large lattice relaxation, e.g. in colour centres. Two different electronic excited states characterized by differing degrees of lattice relaxation are thus separated by a configurational energy barrier (e.g. Fig. 5.12a). Also, Henry and Lang invoked a double well model to account for the observed thermally activated capture cross sections in deep traps in GaP and GaAs (Figs. 5.12b,c). A similar model was used to explain the persistent photoconductivity observed in compound semiconductors such as $Al_xGa_{1-x}$ by Lang and Logan.[53] These cases correspond to an intersection of the configuration coordinate curve of the defect + trapped carrier with that of the defect + free carrier, resulting in the possibility of nonradiative capture by activation over the energy barrier, $E_B$. Both situations differ conceptually from those of type II in that the relaxations are essentially just a stretching or contraction of the existing bonds coupling the lattice to the defect. Hence the large

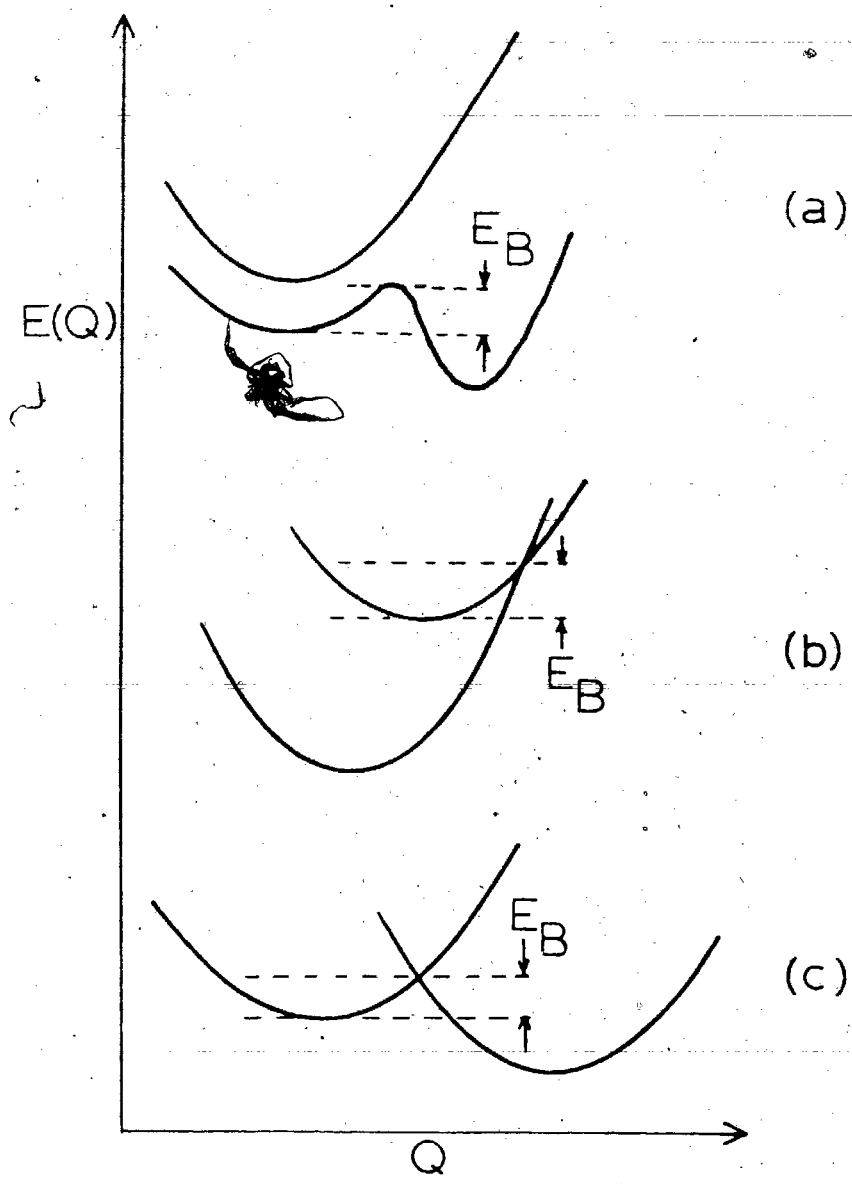


Fig. 5.12

Three different examples of large lattice relaxation models used previously to explain metastable effects in semiconductors. In all three curves the upper level is the conduction band. In (a) the lower level represents a donor which can exist in two metastable configurations[51]. In (b) and (c) the lower level is a deep electron level into which free electrons can be trapped if the energy barrier $E_B$ is thermally overcome[52,53].

relaxation treatment of Engleman and Jortner[54] is generally applicable, in which the two minima of the configuration coordinate diagram are coupled to the same phonon and local lattice coordinate, Q. For such a system, the feedthrough rate is given by:

$$W = W_o \, e^{-E_B/kT^*} \tag{9}$$

where $kT^* = (\hbar\omega/2) \coth (2kT/\hbar\omega)$ is an effective temperature, and $\hbar\omega$ is the energy of the phonon mode coupling to the local lattice coordinate.

This expression reduces to the classically activated Mott limit for high T:

$$W\big|_{T=\infty} = W_o \, e^{-E_B/kT} \tag{10}$$

as in the high T capture data of Henry and Lang[52], and reduces to the quantum mechanical tunnelling limit for low T:

$$W\big|_{T=0} = W_o \, e^{-2E_B/\hbar\omega}, \tag{11}$$

as in the low T limit of their capture results. The data of the above authors were based on studies of deep transition element impurities in GaAs and GaP, for which the coupling was predominantly via lattice phonons of large energy, i.e. 34 meV LO or TO modes, or 10 meV TA modes. For Si, the corresponding values of the peaks in the LO, TO, and TA lattice phonon densities of states are respectively 56.5, 58.5, and 17.8 meV.

The results of Fig. 5.9 demonstrate that the feedthrough rate for the observed Si:Tl data corresponds to the Mott limit with a barrier energy of 20.5 meV and $W_o = 1 \times 10^{12}\ s^{-1}$. The lack of any observed low temperature P,Q,R luminescence limits the tunnelling rate described by (10) to a very low value. A low temperature P,Q,R signal $10^3$ times weaker than the A,B,C lines would be difficult to detect. For this case the feedthrough time constant is given by $\tau_{AP} > 10^3\ \tau_A$. From equation (11) this implies a maximum value of $E_B/\hbar\omega < 12$. With the measured value of $E_B = 20.5$ meV, this would imply $\hbar\omega < 2$ meV. This is a very low phonon energy for which there is little evidence in the phonon replicas of either the P or the A centre luminescence. The very low density of TA states in this energy region make it extremely unlikely that the feedthrough is mediated by lattice phonons, as was the case in all previous studies in which the above treatment has been verified. Most of the systems to which this treatment has been successfully applied have involved defects with relatively high symmetry, i.e. single atom defects which couple only to large energy lattice phonons and would not be expected to support lower energy local mode oscillations. Since the impurity responsible for these lines must consist of more than one constituent, one of which is a relatively massive Tl atom, it is possible that the Si:Tl data could be explained by coupling to a very low energy local mode, of energy $\hbar\omega < 2$ meV, although there is no evidence of such a mode in the spectral data.

The very different nature of the phonon sidebands of the P,Q,R and A,B,C lines are suggestive of quite different binding centre structures. Indeed, Sauer and Weber[55] have concluded from initial Zeeman studies that

the binding centre symmetries are quite different. The above evidence points to a more drastic configurational change than a mere symmetrical contraction or expansion of the surrounding lattice induced by some change in the electronic state of the IBE. The wide differences in the spectral structure would tend to imply some form of lattice relaxation of type II in which a component of the binding centre hops to a different lattice position. The lack of observed tunnelling at low temperatures implies a spatially extended energy barrier.

## Si:In Transient Results

Prior to the results observed as part of this project, the transient behaviour of the P,Q,R lines in Si:In was not well understood. While Mitchard et al.[20] did observe the long lifetimes of these centres, they reported very little temperature dependence of the lines. Their low signal levels allowed them to follow the luminescence decay over two decades or less. Similarly, the initial transient results of Thewalt et al.[22] showed little temperature dependence, due largely to the fact that the luminescence decay was followed over too short a time interval since only a small number of time points were allowed with the particular system used. In both of the above studies a simple exponential decay was observed. The Si:In transient data presented in this project however, were obtained with the computer-based multichannel scaler, capable of recording up to 2000 data points with dwell times of 1 to 500 μs, and which allowed transient data to be readily observed over as many as seven decades of decay. In addition the use of the previously described quenching technique provided

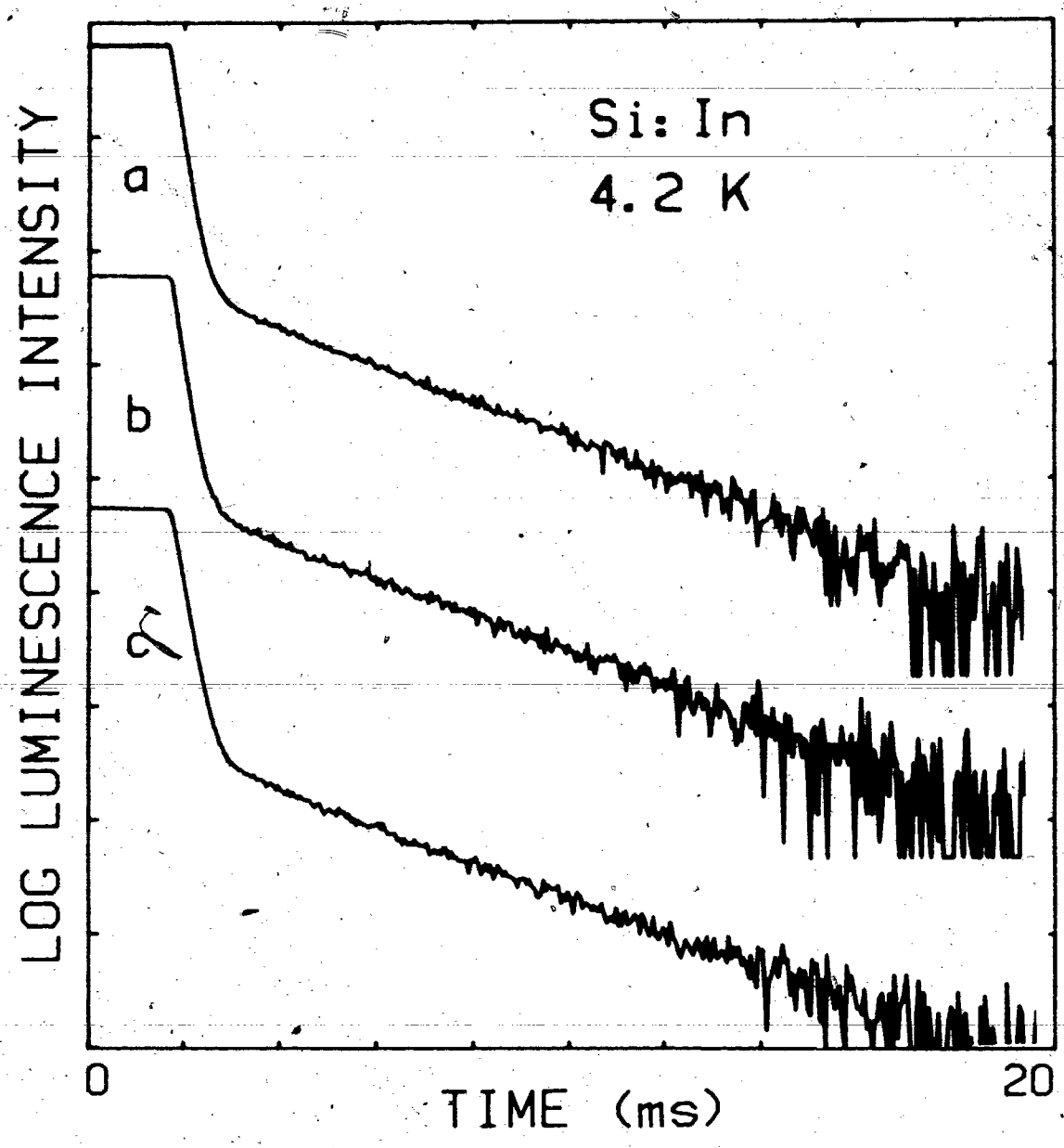


Fig. 5.13

Decay spectra for two different samples of Si:In taken at 4.2K using $Kr^+$ laser excitation. Curves (a) and (b) correspond respectively to the P and R lines of the Si:In 112 samples. Curve (c) corresponds to the P line of the Si:In 24 sample. All curves are identical to within experimental error. Vertical axis markers are decades.

much higher luminescence intensities than those available to Mitchard et al.[20] Count rates had to be limited to average levels of $10^5$ counts per second by reducing the spectrometer aperture in order to avoid saturating the photomultiplier tube with high peak intensities. At these count rates, good statistics were obtained in the order of 10 minutes.

Figure 5.13 represents a summary of the main features of the 4.2 K transient data obtained with $Kr^+$ laser excitation. The decay consists of two exponentials whose time constants differ by an order of magnitude. Previous studies had observed only the fast 200 μs component, completely missing the weaker, much longer lived 3.2 ms component seen in Fig. 5.13. The strongest spectra showed this decay to be exponential over more than two decades. These transient features were sample independent, based on the measurements displayed in Fig. 5.13 taken from two completely unrelated samples, Si:In 24 and Si:In 112. Similar decay curves were also seen in the much weaker Si:In 23 samples. The same features were observed in all phonon replicas (e.g. the local mode replica R, as shown in Fig. 5.13), which rules out the possibility of spurious spectral interference. In addition, the features were not dependent upon excitation power or upon the pulse repetition rate. Several samples were subjected to a range of quench rates from various temperatures, with no discernible effect on the shape of the decay spectra.

The temperature dependence of the photoluminescence decay is summarized in Fig 5.14 for four temperatures in the region from 3 K to 9 K. This data was obtained with the pulsed GaAs laser diode. All data can be expressed to within experimental uncertainty as the sum of two exponentials with temperature dependent time constants, $\tau_L$ and $\tau_S$, and

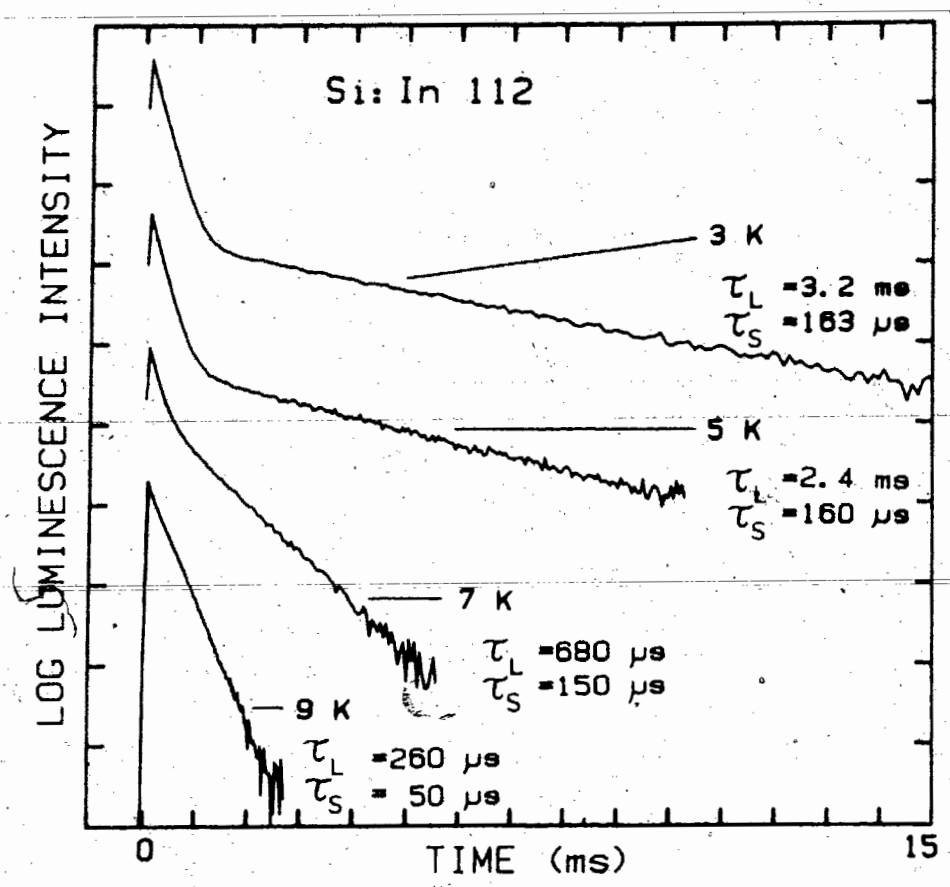


Fig. 5.14

Decay spectra from the P line of the Si:In 112 sample at four representative temperatures. The markers along the vertical axis are decades.

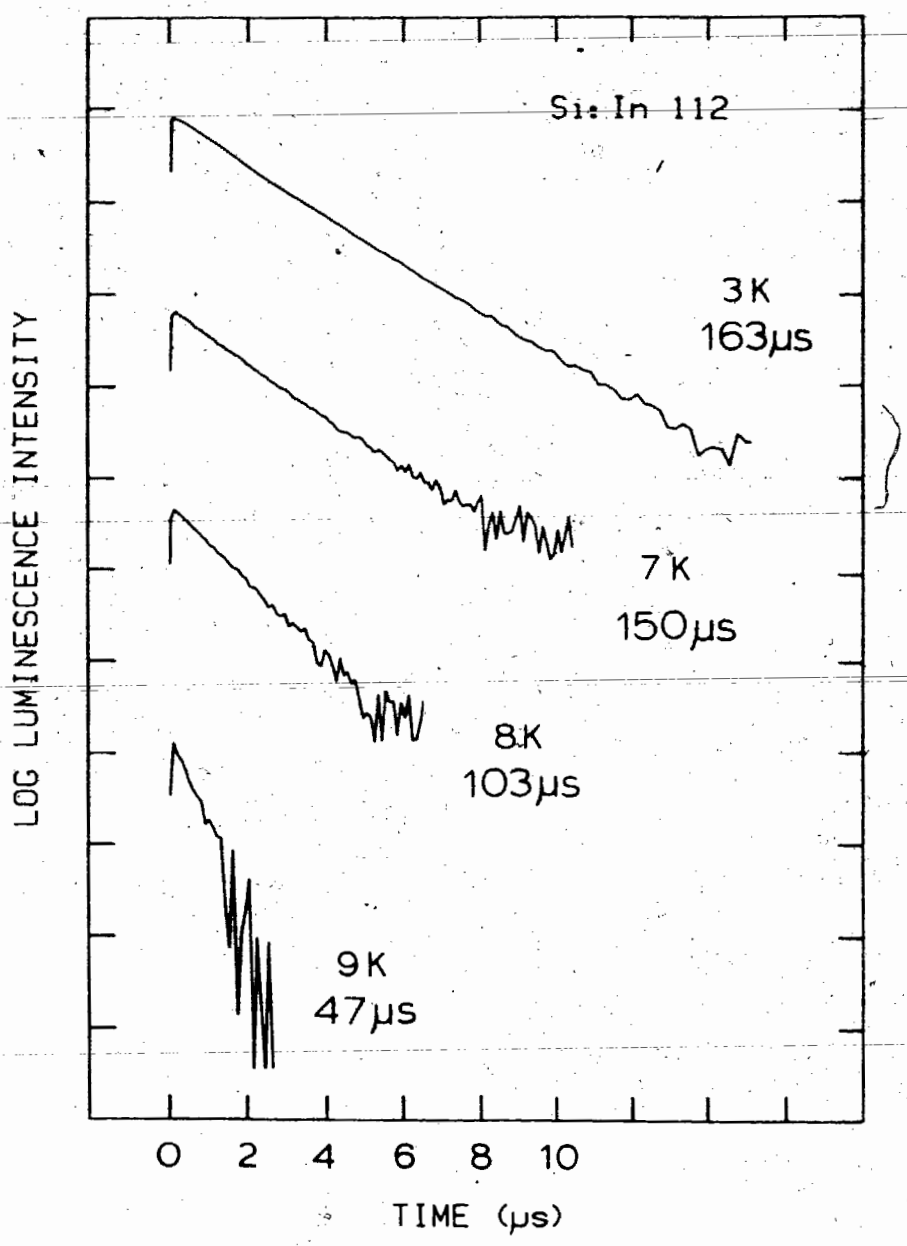


Fig. 5.15

The result of subtracting least squares fits to the long lived portion of the curves shown in Fig. 5.14 from the raw data. The high degree of exponentiality in the resulting curves indicates that only two exponentials contribute to the Si:In decay. Vertical axis markers are decades.

exponential prefactors $I_L$ and $I_S$ corresponding to the intensities of the long-lived and short-lived components extrapolated to t = 0. For a given temperature, $\tau_S$ was obtained by fitting an exponential to the long-lived portion, and subtracting this fit from the data. The resulting subtracted transient spectra are shown at four representative temperatures in Fig. 5.15. For the 3 K data the resulting curve was linear over three orders of magnitude. Even at 9 K, at which temperature $I_S < I_L$, the decay was linear over a full order of magnitude . In the low temperature limit of 1.2K, $\tau_L$ and $\tau_S$ reached the limiting values of 3400 and 163 $\mu$s respectively, with $I_S/I_L \sim 10^3$. The temperature dependence of the lifetimes of the two components is plotted in detail in Fig. 5.16. $\tau_L$ is seen to decrease gradually between 1.2 K to 5.0 K, beyond which point it drops rapidly until reaching the constant value of 230 $\mu$s at T > 10 K, which is maintained up to 20 K. Above 20 K, thermal quenching accounts for the rapid drop in the decay time. $\tau_S$ decreases gradually at first with increasing temperature, then rapidly drops to a value less than the experimental resolution above 10 K. At the same time there is a rapid changeover in the ratio $I_S/I_L$ from $\sim 10^3$ at 1.2 K to a small value ($< 10^{-2}$) above 9 K. The temperature dependence of the ratio $I_S/I_L$ is plotted in Fig. 5.17. The above experimental data are tabulated in Table 5.2.

The fact that these remarkable changes passed unnoticed in previous studies is not surprising, since these earlier measurements did not extend to the long delay times necessary to observe the double exponential behaviour.

The double exponential nature of these decay curves, combined with the rapid nature of the changeover in the transient data as summarized in

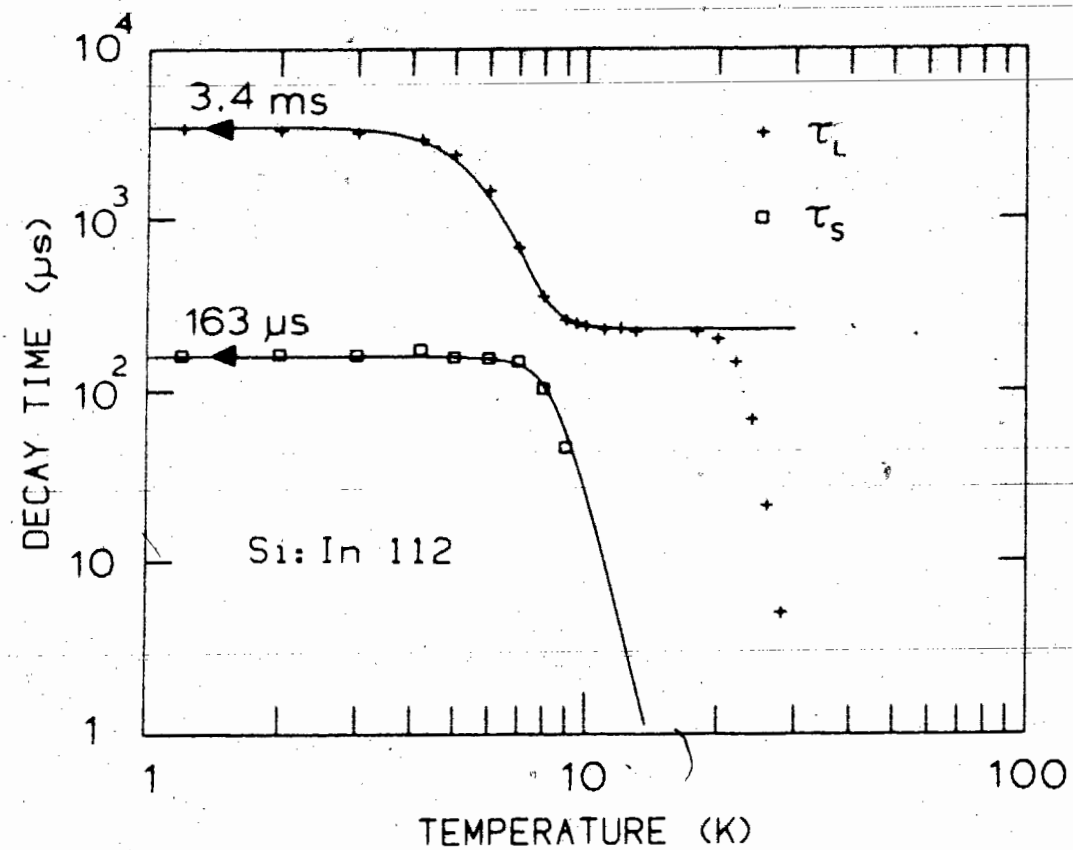


Fig. 5.16

Temperature dependence of the time constants of the two components of the Si:In decay curves, $\tau_L$ and $\tau_S$. The rapid fall of $\tau_L$ above 20K is due to thermal dissociation of the IBE.

Table 5.2

Si:In Transient Results

| T (K) | $\tau_S$ (μs) | $\tau_L$ (ms) | $I_S/I_L$ |
|---|---|---|---|
| 1.2 | 163 | 3.40 | 476 |
| 2.0 | 166 | 3.30 | 248 |
| 3.0 | 163 | 3.20 | 129 |
| 4.2 | 161 | 2.79 | 104 |
| 5.0 | 160 | 2.4 | 90.3 |
| 6.0 | 156 | 1.45 | 26.5 |
| 7.0 | 146 | 0.606 | 5.85 |
| 8.0 | 93 | 0.370 | 1.11 |
| 9.0 | 56 ? | 0.264 | <1 |
| 15.0 | ~0 | 0.230 | 0 |
| 20.0 | | 0.220 | |

Over the region in which the Si:In luminescence shows a double exponential decay behaviour, $\tau_S$ is the time constant of the fast decay component and $\tau_L$ is the time constant of the slow decay component. $I_S$ and $I_L$ are the intensities of these two exponential components extrapolated to t = 0.

Figs. 5.14 and 5.16, were immediately suggestive of some form of binding centre configurational change related to that observed in Si:Tl. It was anticipated that the failure to observe a luminescence system comparable to the A,B,C system might be accounted for by postulating an extremely long radiative lifetime for centres in that configuration. In such a model, the long-lived component observed at low temperatures would corresond to tunnelling from the non-radiative A-type centre to the P,Q,R centre, whose radiative lifetime would correspond to 163 μs, i.e. the low temperature limit of the P,Q,R system decay time. For brevity, these two centres will be referred to as A or P, as in the case of Si:Tl. The Si:In results must be explained by postulating initial exciton capture into both the A and P-centres. Since the initial intensity ratios of the two exponential prefactors at low temperatures (T <4 K) are of the order of $I_S/I_L \sim 10^2$, the initial concentration ratio of A and P-centres is given by :

$$\frac{n_P(0)}{n_A(0)} \sim \frac{I_S\ \tau_A}{I_L\ \tau_{AP}} \sim 10^2 \cdot \frac{163}{3400} \sim 5$$

where $\tau_{AP}$ is taken to be the measured low temperature limit of $\tau_L$. Hence, exciton capture is primarily into the P-type configuration in contrast to the case of Si:Tl. As in the case of the Si:Tl system, these initial concentrations could be due either to the existence of two distinct, but almost degenerate bare binding centres, or to the reconfiguration of the IBE during the capture process. The former case would be described by a configuration coordinate diagram similar to that of the Si:Tl case depicted in Fig. 5.8a, but with the modification that the bare A-centre ground state lie below that of the bare P-centre. From Fig. 5.17, the concentration

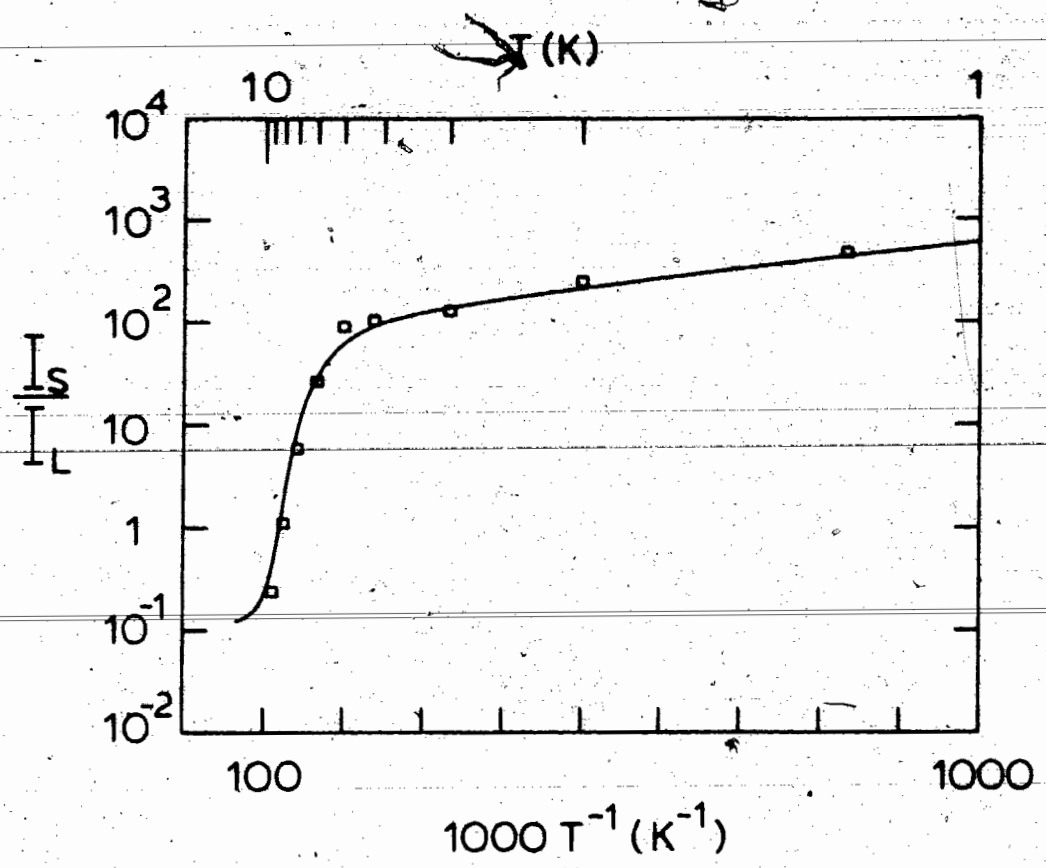


Fig. 5.17

A plot of the ratios of the two t = 0 intensity components, $I_S/I_L$, of the Si:In decay curves, as a function of temperature. The ratio goes from roughly $10^3$ at 1.2K to less than unity above 9K. The solid curve represents the best fit based on the simple rate equation analysis in the text. The predicted flattening of the curve at high T is impossible to verify experimentally since the integrated intensity, $I_S\tau_S$ goes rapidly to zero above 10K.

ratio $n(0)_A/n(0)_P$ is observed to be thermally activated between 1.2 and 4 K, with an energy of 0.2 meV. This could be interpreted either as evidence of a 0.2 meV energy separation of the two bare binding centres as discussed above, or a 0.2 meV activation of the ratio of the capture cross sections. In any case, it would appear that the initial ratio of binding centres does not vary much (less than a factor of 10) over the temperature range of 1.2 to 4 K.

The first effect of an increase in temperature beyond 4 K is a rapid decrease in $\tau_L$ as A-centres are converted to P-centres through thermally assisted tunnelling. As $\tau_L$ becomes shorter, the initial intensity ratio $I_S/I_L$ becomes smaller in such a way as to hold the integrated intensity ratio, equal to the initial ratio of binding centre populations, roughly constant.

The higher temperature results can then be explained in terms of the Si:Tl model but with the condition that $E_X$, the difference in exciton ground state energies for the two centres, be small in comparison with kT above 10 K (i.e. $E_X$ <1 meV) so that feedthrough can occur in both directions at higher temperatures. In the limit of high temperatures, this feedthrough in both directions becomes large and classically activated. In this regime, the feedthrough rates are large enough for the A and P populations to reach thermal equilibrium with relative populations $N_A/N_P = g_A/g_P$, where $g_A$ and $g_P$ are the total effective degeneracy factors of the A and P-centres. After establishing this equilibrium the system decays with a single time constant $\tau_L$ given by:

$$\tau_L = \tau_P \frac{(g_A + g_P)}{g_P} \qquad (12)$$

where $\tau_P = 163\ \mu s$ is the measured low T radiative lifetime of the P-centre, $\tau_L$ is the observed high temperature limit of the P-centre decay time, and the radiative lifetime of the A-centre is treated as essentially infinite. The P-centre decay time actually increases in this regime since more excitons spend time in the nonradiative A-centre configuration. Experimentally, this regime is observed to occur at 10 K, and is maintained up to 20 K, beyond which point thermal breakup of the IBE is observed. Equation (12) fixes the effective degeneracy ratio at $g_P/g_A = 2.3$.

The set of rate equations governing the above description differ from those of the Si:Tl model only in the addition of a term governing feedthrough from P to A. The equations are given by:

$$\frac{dn_A}{dt} = -\frac{n_A}{\tau_A} - \frac{n_A}{\tau_{AP}} + \frac{n_P}{\tau_{PA}} \tag{13}$$

$$\frac{dn_P}{dt} = -\frac{n_P}{\tau_P} + \frac{n_A}{\tau_{AP}} - \frac{n_P}{\tau_{PA}} \tag{14}$$

where $1/\tau_{AP}$ and $1/\tau_{PA}$ represent the transition rates from A to P and P to A respectively, and $\tau_P$ and $\tau_A$ are the respective radiative lifetimes. For completeness, an A-centre radiative decay term is included in equation (13), although $\tau_A$ is assumed to be large in comparison with the P-centre lifetime. While considerable efforts were directed towards the observation at low temperatures of a weak, long lived luminescence system on the high energy side of the P line, nothing was observed. Such a system would have a decay constant equal to that of the long time constant of the P,Q,R lines. Equations (13) and (14) have an exact analytical solution of the form:

$$n_A = A\, e^{-t/\tau_L} + B\, e^{-t/\tau_S} \tag{15}$$

$$n_P = C\, e^{-t/\tau_L} + D\, e^{-t/\tau_S} \tag{16}$$

where A and B are dependent on C and D, and the constants are determined by the boundary conditions, $n_A(t=0) = N_A$ and $n_B(t=0) = N_P$; $N_A$ and $N_P$ are the initial t=0 A and P-type exciton populations respectively. The values of these constants are given in the Appendix.

A computer fit to the $\tau$ vs T data shown in Fig. 5.16 was undertaken based on the use of (11) for the non-classical feedthrough rate. Thus for the A-P feedthrough time constant, the following expression was used:

$$\tau_{AP} = \tau_o\, e^{E_B/kT^*} \tag{17}$$

In this case, the parameters $E_B$ and $\tau_o$ cannot be determined by the experimental data as they were in the Si:Tl results. However, an additional constraint is obtained by assuming that the low temperature A-centre decay rate of $(3400\ \mathrm{ms})^{-1}$ corresponds to the T = 0 tunnelling limit:

$$W = W_o\, e^{-2E_B/\hbar\omega} \tag{18}$$

This constraint then allows the use of $E_B$ and $\tau_o$ as independent fitting parameters which in turn fix the value of $\hbar\omega$.

The expression used for the reverse feedthrough rate was chosen to be of the form:

$$\tau_{PA} = \tau_o \frac{g_P}{g_A} e^{E_B/kT^*} e^{E_X/kT} \tag{19}$$

This form has the property that it gives the correct high T limit:

$$\left.\frac{\tau_{PA}}{\tau_{AP}}\right|_{T=\infty} = \frac{g_P}{g_A} \tag{20}$$

as well as ensuring that for $E_X > 0$, $\tau_{PA}$ tends to infinity as T tends to zero. The computer fit to the $\tau$ vs T data shown in Fig. 5.16 was obtained with $E_B$ = 23 meV, $E_X$ = 0, and $\tau_o = 1 \times 10^{-3}$. From (18), this in turn fixes the value of the phonon frequency $\hbar\omega$ at approximately 2 meV which is the same as the upper limit for previous case of Si:Tl. The value of $E_X \sim 0$ is consistent with the low temperature at which the A to P changeover takes place. The values of $E_B$ and $\tau_o$ which gave reasonable fits were not unique. Good fits were obtained by varying $E_B$ and $\tau_o$ simultaneously between limits of 19 - 24 meV and $10^{-12}$ - $10^{-14}$ s.

A useful test of the validity of the above procedure is provided by a calculation of the temperature dependence of the ratio of the exponential prefactors, $I_S/I_L$ using the above parameters. From (15), $I_S/I_L$ is given by the ratio D/C where D and C are given in the appendix and depend upon $\tau_S$, $\tau_L$ and the initial t=0 concentrations $N_A$ and $N_P$. The resulting fit to the data is given in Fig. 5.17. The low T activation of the ratio $I_S/I_L$ was incorporated by assuming a 0.23 meV activation of the t=0 A-centre to P-centre concentration ratio. The T>4 K behaviour is accurately modelled using the parameters obtained for the $\tau$ vs T fits derived previously. In

particular the ratio $I_S/I_L$ is predicted to change from greater than unity below 6 K to less than unity above 6 K. The set of parameters which best fits both Figs. 5.16 and 5.17 were $E_B$ =23 meV, $E_X$ = 0, and $\tau_o$ = $10^{-13}$ s. The fact that similar parameters gave a good fit to both sets of data safely rules out the possibility that the close lifetime fit was fortuitously due to the use of an unreasonable number of adjustable parameters.

The chief result of the above analysis is the conclusion that the Si:In transient data can be fitted to a rate equation analysis similar to that of the Si:Tl centre but with different assumptions regarding the relative lifetimes and energies of the exciton levels. Similar values of the exciton barrier energy $E_B$ were used in both cases. The feedthrough time constant prefactor $\tau_o$, obtained experimentally in the case of Si:Tl, provided a good fit of the Si:In data also. These similarities offer further evidence that the Si:In and Si:Tl isoelectronic systems share very similar structural properties.

The question of whether or not the 2 meV phonon mode predicted by the above analyses has any physical reality is beyond the scope of the data presented here. It may be that the above description is largely phenomenological, but the validity of the overall rate equation analysis would not be affected if this were the case.

## VI. Summary and Conclusions

The results of transient photoluminescence measurements on several new impurity related luminescence lines in various samples of crystalline Si have confirmed the origin of these lines as due to the recombination of excitons at isoelectronic binding centres. Temperature dependent transient measurements on two sets of lines in Si:Be have verified that both fit into the standard systematics of the j-j coupling model previously applied to isoelectronic defects in other hosts. Absorption measurements on one of these centres permitted for the first time the calculation of the binding centre concentration of an isoelectronic binding centre in Si.

Lifetime measurements on two related sets of lines in samples of Li doped, electron irradiated Si confirm their isoelectronic nature and show some novel similarities with the lines observed in Si:Be. It has been postulated that both pairs of lines bear a relationship to each other which is similar to that between the X-centre acceptors in Si and their simple substitutional counterparts. In this model, the presence of nearest neighbour carbon could lower the central cell potential of an isoelectronic donor, resulting in a weaker, higher energy set of luminescence lines.

Lifetime measurements were reported on an obscure set of intense luminescence lines in Si:Cu which demonstrated their isoelectronic nature. The high degree of coupling to local mode phonons is unprecedented in Si.

In addition, completely novel behaviour has been reported for two isoelectronic luminescence systems in Si:In and Si:Tl. A rate equation analysis based on detailed transient measurements has verified that the

binding centres responsible for both sets of lines undergo a similar process involving some kind of change in configuration which occurs over a narrow temperature interval ($\Delta T \sim 4$ K). Such behaviour is new to the field of photoluminescence studies in semiconductors. The most likely explanation of the effects presented here would appear to involve the rearrangement of one of the binding centre constituents rather than a mere local lattice relaxation as has been the proposed model in the case of many metastable donor level effects. The model of the dynamic tunnelling of hydrogen put forth by Haller et al.[56] to explain an unusual changeover in certain donor and acceptor absorption lines, offers an example of a mobile constituent which can drastically affect the spectral data. Some form of tunnelling is clearly present in the Si:In isoelectronic centres although no detailed model has yet emerged. A complete analysis of this problem must await the application of perturbative techniques, such as Zeeman and stress analysis.

## VII. Appendix: Solution of Si:In Rate Equation

The rate equations for the case of the Si:In model presented previously are given by:

$$\begin{pmatrix} \dot{n}_A \\ \dot{n}_P \end{pmatrix} = \begin{pmatrix} -\alpha & \beta \\ \alpha & -\gamma \end{pmatrix} \begin{pmatrix} n_A \\ n_P \end{pmatrix} = M \begin{pmatrix} n_A \\ n_P \end{pmatrix}$$

where:

$$\alpha = \frac{1}{\tau_A} + \frac{1}{\tau_{AP}} \qquad \beta = \frac{1}{\tau_{PA}}$$

$$\gamma = \frac{1}{\tau_P} + \frac{1}{\tau_{PA}}$$

The solutions are of the form:

$$\begin{pmatrix} n_A \\ n_P \end{pmatrix} = C_S \hat{e}_1 \, e^{\lambda_S t} + C_L \hat{e}_2 \, e^{\lambda_L t}$$

where $\lambda_S$, $\lambda_L$ and $\hat{e}_L$, $\hat{e}_S$ are the eigenvalues and eigenvectors of of M, and $c_S$ and $c_L$ are determined by the boundary conditions. M has eigenvalues given by:

$$-\lambda_S \equiv \frac{1}{\tau_S} = \frac{(\alpha + \gamma) + \sqrt{(\alpha + \gamma)^2 - 4\alpha\,(\gamma - \beta)}}{2}$$

$$-\lambda_L \equiv \frac{1}{\tau_L} = \frac{(\alpha + \gamma) - \sqrt{(\alpha + \gamma)^2 - 4\alpha\,(\gamma - \beta)}}{2}$$

and eigenvectors:

$$\hat{e}_L = \begin{pmatrix} \beta \\ \dfrac{1}{\alpha + \lambda_L} \end{pmatrix} \qquad \hat{e}_S = \begin{pmatrix} \beta \\ \dfrac{1}{\alpha + \lambda_S} \end{pmatrix}$$

Hence the A and P type exciton populations are given by :

$$n_A = C_S(\gamma + \lambda_S)\ e^{-t/\tau_S} + C_L(\gamma + \lambda_L)\ e^{-t/\tau_L}$$

$$n_P = C_S(\alpha)\ e^{-t/\tau_S} + C_L(\alpha)\ e^{-t/\tau_L}$$

with the boundary conditions (at t=0):

$$C_S(\gamma + \lambda_S)\ e^{\lambda_S t} + C_L(\gamma + \lambda_L) = N_A$$

$$C_S(\alpha)\ e^{\lambda_S t} + C_L\ \alpha\ e^{\lambda_L t} = N_P$$

Thus the closed forms for $c_S$ and $c_L$ are given by :

$$C_L = N_A - \frac{N_P}{\alpha}(\gamma + \lambda_S)\frac{1}{(\lambda_L - \lambda_S)} \qquad C_S = \frac{N_P}{\alpha} - C_L$$

which are then simply related to the constants A, B, C, and D referred to in equations 5.15 and 5.16.

## REFERENCES


1 M.A. Lampert, Phys. Rev. Lett. 1,450 (1958).

2 J.R. Haynes, Phys. Rev. Lett. 4,361 (1960).

3 P.J. Dean, J.R. Haynes, W.F. Flood, Phys. Rev. 161, 711 (1967).

5 N.O. Lipari, A. Baldereschi, M.L.W. Thewalt, Solid State Commun. 33, 277 (1980).

4 W. Kohn and J.M. Luttinger, Phys. Rev. 98,915 (1955).

6 D.G. Thomas, J.J. Hopfield, and C.J. Frosch, Phys. Rev. Lett. 15, 857 (1965).

7 J.J. Hopfield, D.G. Thomas, and R.T. Lynch, Phys. Rev. Lett. 17, 312 (1966).

8 P.J. Dean, J.D. Cuthbert, R.T. Lynch, Phys. Rev. 179, 754 (1969).

9 A. Baldereschi, J.J. Hopfield, Phys. Rev. Lett. 28, 171 (1972).

10 D.F. Nelson, J.D. Cuthbert, P.J. Dean, and D.G. Thomas, Phys. Rev. Lett. 17,1262 (1966).

11 J.D. Cuthbert, D.G. Thomas, Phys. Rev. 154, 763 (1967).

12 S.A. Lyon, G.C. Osbourn, D.L. Smith, and T.C. McGill, Solid State Commun. 23,425 (1977).

13 W. Schmid, Phys. Stat. Sol. (b) 84, 529 (1977).

14 J. Weber, W. Schmid, R. Sauer, J. Luminesc. 18/19,93 (1979)-Proc. Int. Conf. Luminesc., Paris, 1978.

15 J. Weber, W. Schmid, R. Sauer, Phys. Rev. B21, 2401 (1980).

16 J.A. Rostworowski and R.R. Parsons, Can. J. Phys. 59, 496 (1981).

17 M.O. Henry, E.C. Lightowlers, N. Killoran, D.J. Dunstan, B.C. Cavenett, J. Phys. C.: Solid State Phys. 14, L255 (1981).

18 L. Canham, G. Davies, E.C. Lightowlers, J. Phys. C.: Solid State Phys. 13, L757 (1980).

19 M.A. Vouk, E.C. Lightowlers, J. Luminesc. 15, 357, (1977).

20 G.S. Mitchard, S.A. Lyon, K.R. Elliot, T.C. McGill, Solid State Commun. 29, 425 (1979).

21 D.H. Brown, S.R. Smith, J. Luminesc. 21, 329 (1980).

22 M.L.W. Thewalt, U.O. Ziemelis, R.R. Parsons, Solid State Commun. 39, 27 (1982).

23 J. Weber, R. Sauer, P. Wagner, J. Luminesc. 24/25, 155 (1981).

24 M.L.W. Thewalt, U.O. Ziemelis, S.P. Watkins, R.R. Parsons, Can. J. Phys., 60,1691 (1981).

25 P. Wagner, J. Weber, R. Sauer, Solid State Commun. 39, 1273 (1981).

26 M.L.W. Thewalt, U.O. Ziemelis, R.R. Parsons, Phys. Rev. B 24, 3655 (1981).

27 R.E. Stahlbush, R.A. Forman, J. Luminesc. 26, 227 (1982).

28 S.P. Watkins, U.O. Ziemelis, M.L.W. Thewalt, R.R. Parsons, Solid State Commun. 43, 687 (1982).

29 M.L.W. Thewalt, S.P. Watkins, U.O. Ziemelis, E.C. Lightowlers, M.O. Henry, Solid State Commun. 44, 573 (1982).

30 S.P. Watkins, M.L.W. Thewalt, T. Steiner, Solid State Commun. to be published.

31 N. Killoran, D.J. Dunstan, M.O. Henry, E.C. Lightowlers, B.C. Cavenett, J. Phys. C: Solid State Phys. 15, 6067 (1982).

32 J. Weber, H. Bauch, and R. Sauer, Phys. Rev. B25, 7688 (1982).

33 R.K. Crouch, J.B. Robertson, T.E. Gilmer, Phys. Rev. 5, 3111 (1972).

34 J.W. Morgan and T.N. Morgan, Phys. Rev. B1,739 (1970).

35 E.U. Condon and G.H. Shortley, "The Theory of Atomic Spectra", Cambridge University Press, 1935.

36 E. Cohen, M.D. Sturge, Phys. Rev. B 15, 1039 (1977).

37 D.L. Dexter, Solid State Physics, edited by F. Seitz and D. Turnbull (Academic Press Inc., New York, 1958) Vol. 6, p. 371.

38 C.E. Jones, D. Schaffer, W. Scott, and R.J. Hager, J. Appl. Phys. 52, 5148 (1981).

39 C.B. Collin, R.O. Carlson, Phys. Rev. 108, 1409 (1957).

40 N.S. Minaev, A.V. Mudryi, V.D. Tkachev, Fiz. Tekh. Poluprovdn. 13,395 (1979) (Sov. Phys.-Semicond. 13, 233 (1979)).

41 J. Weber, P Wagner, Proc. 15th Int. Conf. Physics of Semiconductors, Kyoto, 1980. J. Phys. Soc. Japan 49 (1980), Suppl. A. p. 263.

42 K. Graff and H. Pieper in Semiconductor Silicon 1981, Proc. 4th Int. Symposium on Silicon Materials Science and Technology, edited by H.R. Huff and R.J. Kriegler (The Electrochemical Society, Pennington, New Jersey, 1981), Vol. 81-5, p. 331.

43 T.N. Morgan, B. Welber, R.N. Bhargava, Phys. Rev. 166, 751 (1968).

44 C.H. Henry, P.J. Dean, J.D. Cuthbert, Phys. Rev. 166, 754 (1968).

45 W. Scott, J.L. Schmit, Appl. Phys. Lett. 33(4), 294 (1978).

46 J.M. Langer, Proc. 15th Int. Conf. Physics of Semiconductors, Kyoto, 1980. J. Phys. Soc. Japan 49 (1980), Suppl. A, p. 207.

47 D.V. Lang, Proc. 15th Int. Conf. Phys. of Semiconductors, Kyoto, 1980. J. Phys. Soc. Japan 49 (1980), Suppl. A, p. 215.

48 Porowski, M. Konczykowski, J. Chroboczek, Phys. Stat. Sol. (a) 63, 291 (1974).

49 L. Dmowski, M. Konczykowski, R. Piotrzkowski, S. Porowski, Phys. Stat. Sol. (b) 73, K131 (1976).

50 M. Baj, L. Dmowski, M. Konczykowski, S. Porowski, Phys. Stat. Sol. (a) 33, 421 (1976).

51 U. Piekara, J.M. Langer, B. Krukowska-Fulde, Solid State Commun. 23, 563 (1977).

52 C.H. Henry, D.V. Lang, Phys. Rev. B15, 989 (1977).

53 D.V. Lang, R.A. Logan, Phys. Rev. Lett. 39, 635 (1977).

54 R. Engleman, J. Jortner, Mol. Phys. 18, 145 (1970).

55 R. Sauer and J. Weber, Proc. 12th Int. Conf. on Defects in Semiconductors, Amsterdam, 1982.

56 E.E. Haller and L.M. Falicov, Phys. Rev. Lett. 41, 1192 (1978).